

Sharp Bounds for Treatment Effect Generalization under Outcome Distribution Shift

Amir Asiaee

AMIR.ASIAEETAHERI@VUMC.ORG

Samhita Pal

SAMHITA.PAL@VUMC.ORG

Cole Beck

COLE.BECK@VUMC.ORG

Department of Biostatistics, Vanderbilt University Medical Center, Nashville, TN, USA

Jared D. Huling

HULING@UMN.EDU

Division of Biostatistics and Health Data Science, University of Minnesota, Minneapolis, MN, USA

Abstract

Generalizing treatment effects from a randomized trial to a target population requires the assumption that potential outcome distributions are invariant across populations after conditioning on observed covariates. This assumption fails when unmeasured effect modifiers are distributed differently between trial participants and the target population. We develop a sensitivity analysis framework that bounds how much conclusions can change when this transportability assumption is violated. Our approach constrains the likelihood ratio between target and trial outcome densities by a scalar parameter $\Lambda \geq 1$, with $\Lambda = 1$ recovering standard transportability. For each Λ , we derive sharp bounds on the target average treatment effect—the tightest interval guaranteed to contain the true effect under all data-generating processes compatible with the observed data and the sensitivity model. We show that the optimal likelihood ratios have a simple threshold structure, leading to a closed-form greedy algorithm that requires only sorting trial outcomes and redistributing probability mass. The resulting estimator runs in $O(n \log n)$ time and is consistent under standard regularity conditions. Simulations demonstrate that our bounds achieve nominal coverage when the true outcome shift falls within the specified Λ , provide substantially tighter intervals than worst-case bounds, and remain informative across a range of realistic violations of transportability.

Keywords: Generalizability; Transportability; Sensitivity analysis; Partial identification; Randomized trials; Treatment effect heterogeneity

1. Introduction

Randomized trials are the gold standard for estimating causal effects in a well-defined study population, but they are rarely the last word for decision-making in practice. Clinicians, regulators, and health systems want to know whether a treatment that works in a trial will have similar benefits in a target population whose covariate distribution, care pathways, or adherence patterns may differ from those of trial participants. This is the problem of *generalization* or *transportability* of trial results (Stuart et al., 2011; Dahabreh and Hernán, 2019; Pearl and Bareinboim, 2011). Formally, the target estimand is the average treatment effect in a target population, while the data available come from a randomized trial and, often, a separate sample of baseline covariates from the target population.

A now-standard approach assumes that, after conditioning on baseline covariates, potential outcomes are invariant across trial and target populations. Under this assumption, sometimes called *outcome transportability* or *conditional exchangeability over populations*, one can estimate the target effect by combining trial outcomes with trial and target covariate distributions, for example through outcome modeling or inverse probability weighting (Stuart et al., 2011; Dahabreh and

(Hernán, 2019; Bareinboim and Pearl, 2016). In practice, however, it is unlikely that the available covariates capture all effect modifiers that differ between populations. When unmeasured moderators are imbalanced between the trial and the target, the assumption of conditional outcome invariance fails, and generalization procedures can yield misleadingly precise point estimates.

This concern has motivated a growing literature on *sensitivity analysis for generalizability*, which seeks to quantify how conclusions could change under plausible violations of outcome transportability. Existing methods typically introduce bias or sensitivity functions that parameterize the difference between potential outcome means in trial participants and the target population, conditional on covariates (Nguyen et al., 2018; Dahabreh et al., 2023; Huang, 2024). These approaches provide important insight, but they usually operate at the level of conditional mean outcomes and often require researchers to reason directly about unobserved modifiers or specify parametric forms for the bias. At the same time, there is a rich line of work on sensitivity analysis for unmeasured confounding in observational studies, most notably marginal sensitivity models that bound the odds ratio of treatment assignment with and without unmeasured confounders (Tan, 2006; Zhao et al., 2019; Dorn and Guo, 2022). That literature has produced sharp partial identification results and scalable algorithms, but it focuses on deviations in the treatment assignment mechanism within a single population rather than deviations in outcome distributions across populations.

Our goal in this paper is to bring these two strands together. We study generalization from a randomized trial to a target population when the standard conditional outcome transportability assumption fails because of unmeasured moderators that are differentially distributed between the two populations. Instead of modeling the missing moderators directly, we characterize all target outcome distributions that are compatible with the observed trial data and an interpretable bound on how much the conditional outcome distribution can shift between the trial and target. This leads to a simple *outcome-shift sensitivity model*, which plays a role analogous to the marginal sensitivity model of Tan (2006), but applied to the outcome distribution rather than the treatment assignment mechanism.

Concretely, we assume that, for each treatment value and covariate vector, the conditional density of the outcome in the target population is absolutely continuous with respect to the corresponding conditional density in the trial, with likelihood ratio bounded by a scalar sensitivity parameter $\Lambda \geq 1$. When $\Lambda = 1$, the model reduces to standard outcome transportability. As Λ increases, we allow progressively larger departures, in the sense that the log-likelihood ratio between target and trial outcome distributions is bounded in absolute value by $\log \Lambda$ at each (A, X) . For each fixed Λ , we derive the sharp identified set for the target average treatment effect—the smallest interval that must contain the true target effect among all data-generating processes compatible with the observed trial data and the sensitivity model.

Our analysis yields two main methodological contributions:

- **Sharp population-level bounds.** We give a convex characterization of the identified set for target mean potential outcomes and the target ATE under the outcome-shift sensitivity model. We show that the extremal outcome distributions have a simple threshold structure: the optimal likelihood ratio takes only the boundary values Λ^{-1} and Λ , switching at a single outcome threshold. This yields closed-form expressions for the sharp bounds and clarifies how interval width depends on Λ and the variability of trial outcomes.
- **A simple estimation algorithm.** At the sample level, we derive a discrete optimization formulation for the worst-case target means and show that the corresponding linear programs

admit a greedy closed-form solution. The algorithm requires only sorting trial outcomes, computing generalization weights, and redistributing probability mass toward extreme outcomes subject to the likelihood ratio constraint. This yields $O(n \log n)$ estimators for the bounds, with consistency following from standard empirical process arguments.

2. Related Work

Generalization and transportability. There is a substantial literature on extending inferences from randomized trials to target populations. Early work by [Stuart et al. \(2011\)](#) emphasized design and analysis strategies that align trial participants with the target population through covariate balance diagnostics and reweighting. The potential outcomes framework for generalizability and transportability was developed in [Dahabreh and Hernán \(2019\)](#); [Dahabreh et al. \(2020\)](#), which clarify nested and non-nested study designs and describe identification conditions such as conditional mean transportability. [Pearl and Bareinboim \(2011\)](#) and [Bareinboim and Pearl \(2016\)](#) provide a graphical approach to transportability using causal diagrams. Recent reviews survey methods for translating trial findings to real-world settings and offer practical guidance ([Degtiar and Rose, 2023](#); [Ling et al., 2023](#); [Colnet et al., 2024](#)).

Most of this literature assumes that, after adjusting for observed covariates, potential outcome distributions are invariant between trial and target, and focuses on efficient and robust estimation of the corresponding target effect. In contrast, our work starts from the premise that this assumption may fail because of unmeasured effect modifiers whose distribution differs between populations. We ask what can be learned about the target effect from trial data and the target covariate distribution alone, once we allow controlled deviations from outcome transportability.

Sensitivity analysis for unmeasured confounding. Sensitivity analysis for violations of unconfoundedness has a long history in observational studies ([Rosenbaum, 2002](#)). Among many proposals, marginal sensitivity models have attracted recent attention because they yield tractable partial identification problems and admit sharp bounds on causal effects. In the original formulation of [Tan \(2006\)](#), the model bounds the odds ratio of treatment assignment when conditioning on both observed covariates and a latent unmeasured confounder. Subsequent work derived sharp bounds for average treatment effects ([Dorn and Guo, 2022](#)) and developed estimators with strong robustness guarantees ([Zhao et al., 2019](#)). Other authors proposed related sensitivity models based on f -divergence constraints or alternative parameterizations ([Franks et al., 2020](#); [Frauen et al., 2023](#)).

This line of work is conceptually close to ours: we also use a likelihood ratio bound with a scalar sensitivity parameter and derive sharp bounds via convex optimization. The key difference is the object to which the bound is applied. In the marginal sensitivity literature, the constraint is placed on the treatment assignment mechanism within a single population. In our outcome-shift model, the constraint is placed on the conditional outcome distribution across populations, while the treatment mechanism is randomized in the trial. This change in perspective aligns the model with the specific failure mode of generalization that arises from unmeasured effect modification.

Sensitivity analysis for generalization. Several authors have proposed sensitivity analyses tailored specifically to the problem of generalizing trial results. [Nguyen et al. \(2018\)](#) considered settings where an effect modifier is observed in the trial but not in the target sample, and developed methods that express the bias in terms of the unobserved effect modifier distribution. More recently, [Dahabreh et al. \(2023\)](#) proposed a bias function approach that parameterizes violations

of conditional mean transportability through the difference between potential outcome means in randomized and non-randomized individuals, and [Huang \(2024\)](#) introduced a sensitivity analysis based on reweighting estimators that decomposes bias into interpretable components related to effect modification and covariate imbalance.

Our work is closest in spirit to [Dahabreh et al. \(2023\)](#) and [Huang \(2024\)](#), in that we model violations of outcome transportability rather than violations of treatment or sampling mechanisms. However, their approaches operate at the level of conditional means or bias decompositions, whereas our outcome-shift model constrains the full conditional outcome distribution via likelihood ratios. This distributional perspective permits a direct convex characterization of the sharp identified set and yields an extremely simple greedy algorithm for computing sample bounds. In addition, our framework is agnostic about how generalization weights are obtained and can be combined with any existing method for adjusting covariate shift.

Overall, our outcome-shift sensitivity model appears to be new in the context of generalization. It borrows technical ideas from the marginal sensitivity literature for observational studies—particularly the use of likelihood ratio bounds and convex optimization to obtain sharp bounds—but applies them to the outcome channel and to cross-population transportability. To our knowledge, no existing method provides sharp, distributional sensitivity bounds for target average treatment effects under likelihood ratio constraints on outcome distributions, together with a closed-form algorithm that reduces to sorting and reweighting trial outcomes.

3. Problem Formulation and Notation

We adopt the potential outcomes framework for multi-population causal inference, following [Dahabreh and Hernán \(2019\)](#) with notation adapted for our sensitivity analysis. Let $S \in \{r, o\}$ index the *source* randomized trial ($S = r$) and the *target* population ($S = o$). For unit i in population s , we observe a covariate vector $X_i^s \in \mathcal{X} \subset \mathbb{R}^p$, a binary treatment $A_i^s \in \{-1, +1\}$, and an outcome $Y_i^s \in \mathcal{Y} \subset \mathbb{R}$. Potential outcomes are denoted $(Y_i(+1), Y_i(-1))$, with the usual consistency assumption $Y_i = Y_i(A_i)$.

Throughout, we use the study indicator $s \in \{r, o\}$ as a superscript to denote quantities specific to each population. When we write P^s , $\mathbb{E}^s[\cdot]$, or μ_a^s , this should be understood as the distribution, expectation, or parameter *conditional on membership in study s* —that is, we are characterizing the data-generating process within each population separately.

For treatment level $a \in \{-1, +1\}$, we define the conditional and marginal mean potential outcomes in population s as $\mu_a^s(x) := \mathbb{E}^s[Y(a) | X = x]$ and $\mu_a^s := \mathbb{E}^s[Y(a)]$. The average treatment effect (ATE) in population s is $\tau^s := \mu_{+1}^s - \mu_{-1}^s = \mathbb{E}^s[Y(+1) - Y(-1)]$. Our goal is to *generalize* the trial-based treatment effect to the target population—specifically, to learn about $\tau^o = \mathbb{E}^o[Y(+1) - Y(-1)]$ —using data from the trial together with covariate information from the target population.

We observe an i.i.d. sample $\mathcal{D}^r := \{(X_i^r, A_i^r, Y_i^r)\}_{i=1}^{n^r}$ from the trial, where treatment is randomized, and a separate i.i.d. sample of covariates $\mathcal{D}^o := \{X_j^o\}_{j=1}^{n^o}$ from the target population. Crucially, we do not observe outcomes or treatment assignments in the target sample, so the conditional outcome distribution in the target, $P^o(Y | A, X)$, is not directly identified from the data.

3.1. Identification under standard transportability.

To isolate the role of outcome shift, we assume the usual conditions for internal validity of the trial.

Assumption 1 (Trial internal validity) *For the trial population $S = r$:*

- (i) *Consistency:* $Y = Y(A)$ almost surely.
- (ii) *Randomization:* $(Y(+1), Y(-1)) \perp A \mid X, S = r$.
- (iii) *Positivity:* there exists $\eta > 0$ such that $\mathbb{P}^r(A = a \mid X = x) \geq \eta$ for all $a \in \{-1, +1\}$ and almost all x .

Under Assumption 1, the conditional mean potential outcome is identified from trial data as $\mu_a^r(x) = \mathbb{E}^r[Y \mid A = a, X = x]$.

No outcome shift. The standard approach to generalization further assumes *outcome transportability*: the conditional distribution of potential outcomes is identical across populations,

$$P^r(Y(a) \mid X = x) = P^o(Y(a) \mid X = x) \quad \text{for all } x \text{ and } a, \quad (1)$$

sometimes written compactly as $Y(a) \perp S \mid X$ (Pearl and Bareinboim, 2011; Bareinboim and Pearl, 2016). Under this assumption, combining trial outcomes with the target covariate distribution identifies the target effect. Let $w(x) := dP^o/dP^r(x)$ denote the density ratio between the target and trial covariate distributions. Then

$$\tau^o = \mathbb{E}^o[\mu_{+1}^r(X) - \mu_{-1}^r(X)] = \mathbb{E}^r[w(X) \cdot (\mu_{+1}^r(X) - \mu_{-1}^r(X))]. \quad (2)$$

This identity suggests two estimation strategies (Stuart et al., 2011; Dahabreh and Hernán, 2019). The *outcome modeling* approach fits regression models $\hat{\mu}_a^r(x)$ on trial data and averages over the target covariate sample: $\hat{\tau}_{\text{om}}^o = (n^o)^{-1} \sum_{j=1}^{n^o} [\hat{\mu}_{+1}^r(X_j^o) - \hat{\mu}_{-1}^r(X_j^o)]$. The *inverse probability weighting* approach estimates the density ratio $\hat{w}(x)$ typically via logistic regression of the study indicator S on X using pooled data and computes arm-specific weighted means, $\hat{\mu}_{a,\text{ipw}}^o := \frac{\sum_{i=1}^{n^r} \hat{w}(X_i^r) \mathbf{1}\{A_i^r=a\} Y_i^r}{\sum_{i=1}^{n^r} \hat{w}(X_i^r) \mathbf{1}\{A_i^r=a\}}$, then forms $\hat{\tau}_{\text{ipw}}^o := \hat{\mu}_{+1,\text{ipw}}^o - \hat{\mu}_{-1,\text{ipw}}^o$, with denominators computed separately within each arm.

In practice, outcome transportability (1) may fail even when selection into the trial and treatment assignment are well controlled. This occurs whenever unmeasured effect modifiers have different distributions across populations. Our goal is to relax (1) and develop a sensitivity model that quantifies how violations of outcome transportability affect conclusions about τ^o .

3.2. Unmeasured effect modification

To understand when and why outcome transportability (1) fails, it helps to consider a structural model for potential outcomes. Suppose $Y(a) = m_a(X, U, \varepsilon)$, $a \in \{-1, +1\}$, where U is a (possibly multidimensional) unobserved effect moderator and ε is idiosyncratic noise. We impose no restriction on the joint distribution of (X, U, ε) beyond measurability and integrability, and we keep the structural functions m_a fixed across populations. Critically, we allow the conditional distribution of U given X to differ between trial and target: $P^r(U \mid X) \neq P^o(U \mid X)$. This is the key violation: even after conditioning on observed covariates X , the distribution of the unobserved moderator U may differ across populations.

Under Assumption 1, the conditional mean potential outcome in population s is $\mu_a^s(x) = \int m_a(x, u, \varepsilon) dP^s(u, \varepsilon \mid X = x)$. Integrating out ε and defining $\bar{m}_a(x, u) := \mathbb{E}[m_a(x, u, \varepsilon) \mid$

$X = x, U = u]$, we obtain $\mu_a^s(x) = \int \bar{m}_a(x, u) dP^s(u \mid X = x)$. The *conditional outcome shift* at covariate value x and treatment a is

$$\Delta_a(x) := \mu_a^o(x) - \mu_a^r(x) = \int \bar{m}_a(x, u) d(P^o - P^r)(u \mid X = x), \quad (3)$$

which is nonzero whenever the modifier distribution differs across populations in directions correlated with $\bar{m}_a(x, \cdot)$.

A simple example clarifies the mechanics. Suppose the conditional mean is linear in a scalar U : $\mathbb{E}[Y(a) \mid X = x, U = u] = \mu_a^r(x) + \beta_a(x) \cdot u$. Then (3) implies $\Delta_a(x) = \beta_a(x)(\mathbb{E}^o[U \mid X = x] - \mathbb{E}^r[U \mid X = x])$, an omitted-variable-bias decomposition for external validity [Nguyen et al. \(2018\)](#); [Huang \(2024\)](#). Here, the outcome shift is driven by two factors: the strength of effect modification $\beta_a(x)$, and the difference in the conditional distribution of U between populations. If either is zero, transportability holds. But in general, neither $\beta_a(x)$ nor the shift in $P^s(U \mid X)$ is identified from observed data.

4. Outcome-Shift Sensitivity Model

Rather than modeling the unobserved moderator U directly, we take an agnostic approach: we bound the discrepancy between outcome distributions in the trial and target populations using a likelihood ratio constraint. This parallels marginal sensitivity models for unmeasured confounding ([Tan, 2006](#); [Zhao et al., 2019](#)), but applies the bound to the outcome rather than treatment assignment.

4.1. The sensitivity model

Let $f^s(y \mid a, x)$ denote the conditional density of Y given $(A = a, X = x)$ in population $s \in \{r, o\}$. Under randomization in the trial, $f^r(y \mid a, x)$ is identified from the observed data $(Y, A, X, S = r)$.

Definition 2 (Outcome-shift sensitivity model) *Fix a sensitivity parameter $\Lambda \geq 1$. We say that the pair (P^r, P^o) satisfies the outcome-shift sensitivity model with parameter Λ if for each $a \in \{-1, +1\}$ and almost all x , the likelihood ratio*

$$r_a(x, y) := \frac{f^o(y \mid a, x)}{f^r(y \mid a, x)}$$

satisfies:

- (i) (Bounded likelihood ratio) $\Lambda^{-1} \leq r_a(x, y) \leq \Lambda$ for all $y \in \mathcal{Y}$;
- (ii) (Normalization) $\mathbb{E}^r[r_a(X, Y) \mid X, A = a] = \int r_a(x, y) f^r(y \mid a, x) dy = 1$.

The normalization condition simply ensures that $f^o(\cdot \mid a, x)$ integrates to one. Together, the two conditions imply $f^o(y \mid a, x) = r_a(x, y) f^r(y \mid a, x)$ with $\Lambda^{-1} \leq r_a(x, y) \leq \Lambda$.

The sensitivity parameter Λ controls the degree of departure from transportability. When $\Lambda = 1$, the model enforces $f^o(\cdot \mid a, x) = f^r(\cdot \mid a, x)$, recovering the standard transportability assumption (1). As Λ increases, progressively larger outcome shifts are permitted. For interpretation, $\Lambda = 2$ means the target population can have at most twice (or at least half) the density of any outcome value compared to the trial, conditional on (A, X) .

Given $r_a(x, y)$, the conditional mean potential outcome in the target population is

$$\mu_a^o(x) = \int y f^o(y | a, x) dy = \int y r_a(x, y) f^r(y | a, x) dy = \mathbb{E}^r[Y \cdot r_a(X, Y) | A = a, X = x], \quad (4)$$

and the marginal mean is $\mu_a^o = \mathbb{E}^o[\mu_a^o(X)]$. Since $r_a(x, y)$ is not identified from data, neither is μ_a^o . Our goal is to characterize the set of values μ_a^o can take as r_a ranges over all functions satisfying Definition 2.

To connect this to estimation from trial data, let $w(x) := dP^o/dP^r(x)$ denote the density ratio between target and trial covariate distributions, and let $\pi^r(a | x)$ denote the (known) trial randomization probability. The target mean can be written as an expectation over the trial distribution:

$$\mu_a^o = \mathbb{E}^o[\mu_a^o(X)] = \mathbb{E}^r[w(X) \cdot \mu_a^o(X)] = \mathbb{E}^r\left[w(X) \cdot r_a(X, Y) \cdot Y \cdot \frac{\mathbf{1}\{A = a\}}{\pi^r(a | X)}\right]. \quad (5)$$

This identity is key for estimation: it expresses the target quantity as a weighted average of trial outcomes, where the weights combine the covariate shift correction $w(X)$, the outcome shift $r_a(X, Y)$, and the inverse propensity weight $\mathbf{1}\{A = a\}/\pi^r(a | X)$. Since r_a is unknown, we optimize over admissible likelihood ratios to obtain bounds.

4.2. Sharp identification bounds

For a fixed $\Lambda \geq 1$, define the class of admissible likelihood ratio functions

$$\mathcal{R}_a(\Lambda) := \left\{ r_a : \mathcal{X} \times \mathcal{Y} \rightarrow \mathbb{R}_+ \mid \Lambda^{-1} \leq r_a(x, y) \leq \Lambda, \mathbb{E}^r[r_a(X, Y) | X, A = a] = 1 \text{ a.s.} \right\}.$$

The identified set for μ_a^o is $\mathcal{M}_a(\Lambda) := \{\mu_a^o(r_a) : r_a \in \mathcal{R}_a(\Lambda)\}$, and the identified set for the target ATE is $\mathcal{T}(\Lambda) := \{\mu_{+1}^o(r_{+1}) - \mu_{-1}^o(r_{-1}) : r_a \in \mathcal{R}_a(\Lambda)\}$.

To characterize these sets, we first derive bounds on the conditional mean $\mu_a^o(x)$ for fixed (x, a) , then aggregate over the covariate distribution. Define the optimization problems

$$\mu_a^{o,+}(x; \Lambda) := \sup_{r_a \in \mathcal{R}_a(\Lambda)} \int y r_a(x, y) f^r(y | a, x) dy, \quad (6)$$

$$\mu_a^{o,-}(x; \Lambda) := \inf_{r_a \in \mathcal{R}_a(\Lambda)} \int y r_a(x, y) f^r(y | a, x) dy. \quad (7)$$

Structure of optimal solutions. The optimization problems (6)–(7) have a special structure: the objective is linear in the likelihood ratio $r_a(x, y)$, and the constraint set is defined by box constraints plus a single linear equality (normalization). A standard result in linear programming implies that optimal solutions to such problems take extreme values—the likelihood ratio equals either Λ^{-1} or Λ almost everywhere, rather than intermediate values.

To build intuition, consider the maximization problem for $\mu_a^o(x)$. We seek a reweighting of the trial outcome distribution that places as much probability mass as possible on large outcome values. The likelihood ratio $r_a(x, y)$ acts as a redistributor of probability: setting $r_a(x, y) = \Lambda$ inflates the probability of outcome y by a factor of Λ , while $r_a(x, y) = \Lambda^{-1}$ deflates it. The normalization constraint enforces that total probability remains one, so inflation at some values must be offset by deflation elsewhere.

Given this trade-off, the optimal strategy is clear: inflate the largest outcomes as much as possible ($r_a = \Lambda$) and deflate the smallest outcomes as much as possible ($r_a = \Lambda^{-1}$). Any intermediate value of r_a wastes capacity that could be better allocated to the extremes. The following lemma formalizes this.

Lemma 3 (Threshold structure) *Fix x and a , and suppose $Y \mid (A = a, X = x, S = r)$ has support contained in a bounded interval $[L, U]$. Any maximizer of (6) takes the threshold form $r_a^*(x, y) = \Lambda$ for $y > t$, $r_a^*(x, y) = \Lambda^{-1}$ for $y < t$, and $r_a^*(x, t) = r_0 \in [\Lambda^{-1}, \Lambda]$, for some threshold $t \in [L, U]$ determined by the normalization constraint. For the minimization problem (7), the optimal solution has the reversed form. The proof is given in Appendix A.1.*

Lemma 3 implies that the conditional identified set for $\mu_a^o(x)$ is the interval $[\mu_a^{o,-}(x; \Lambda), \mu_a^{o,+}(x; \Lambda)]$, with endpoints attained by threshold likelihood ratios. Aggregating over the covariate distribution yields sharp bounds on the marginal quantities.

Theorem 4 (Sharp bounds for the target ATE) *Suppose Assumption 1 holds, $|Y| \leq C$ almost surely in both populations, and (P^r, P^o) satisfies the outcome-shift sensitivity model with parameter $\Lambda \geq 1$. Then the identified set for the target mean potential outcome is*

$$\mathcal{M}_a(\Lambda) = [\mu_a^{o,-}(\Lambda), \mu_a^{o,+}(\Lambda)], \quad \text{where} \quad \mu_a^{o,\pm}(\Lambda) := \mathbb{E}^o[\mu_a^{o,\pm}(X; \Lambda)].$$

The identified set for the target ATE is $\mathcal{T}(\Lambda) = [\tau^{o,-}(\Lambda), \tau^{o,+}(\Lambda)]$, with $\tau^{o,-}(\Lambda) := \mu_{+1}^{o,-}(\Lambda) - \mu_{-1}^{o,+}(\Lambda)$, $\tau^{o,+}(\Lambda) := \mu_{+1}^{o,+}(\Lambda) - \mu_{-1}^{o,-}(\Lambda)$. These bounds are sharp: for every value in the interval, there exists a pair (P^r, P^o) satisfying the sensitivity model and consistent with the observed trial data for which the target ATE equals that value. The proof is provided in Appendix A.2.

Theorem 4 establishes that the outcome-shift sensitivity model yields a one-dimensional sensitivity analysis indexed by Λ . When $\Lambda = 1$, we recover point identification under standard transportability: $\tau^{o,-}(1) = \tau^{o,+}(1) = \tau^o$. As $\Lambda \rightarrow \infty$, the interval $\mathcal{T}(\Lambda)$ expands toward the range of values consistent with the trial data and covariate distribution alone, with no restriction on outcome transportability.

5. Estimation

We now derive sample analogues of the sharp bounds in Theorem 4 and provide an efficient algorithm for computing them.

5.1. Discrete optimization formulation

Fix a treatment level $a \in \{-1, +1\}$ and let $\mathcal{I}_a := \{i \in \{1, \dots, n^r\} : A_i^r = a\}$ denote the indices of units in the trial receiving treatment a , with $n_a := |\mathcal{I}_a|$. Let $\hat{w}_i := \hat{w}(X_i^r)$ be estimated generalization weights (e.g., from logistic regression of the study indicator S on covariates X using pooled data). Define normalized baseline weights

$$p_i^{(a)} := \frac{\hat{w}_i}{\sum_{j \in \mathcal{I}_a} \hat{w}_j}, \quad i \in \mathcal{I}_a. \quad (8)$$

These weights sum to one and represent the trial outcome distribution reweighted to match the target covariate distribution.

In the finite-sample setting, the outcome-shift sensitivity model reduces to finding multipliers $\lambda_i^{(a)} \in [\Lambda^{-1}, \Lambda]$ such that the reweighted probabilities $q_i^{(a)} := p_i^{(a)} \lambda_i^{(a)}$ sum to one. The sample bounds on the target mean solve the linear programs

$$\hat{\mu}_a^{o,+}(\Lambda) := \max_{\lambda} \sum_{i \in \mathcal{I}_a} p_i^{(a)} \lambda_i^{(a)} Y_i^r, \quad \hat{\mu}_a^{o,-}(\Lambda) := \min_{\lambda} \sum_{i \in \mathcal{I}_a} p_i^{(a)} \lambda_i^{(a)} Y_i^r, \quad (9)$$

subject to $\Lambda^{-1} \leq \lambda_i^{(a)} \leq \Lambda$ for all $i \in \mathcal{I}_a$ and $\sum_{i \in \mathcal{I}_a} p_i^{(a)} \lambda_i^{(a)} = 1$. The sample ATE bounds are then

$$\hat{\tau}^{o,-}(\Lambda) := \hat{\mu}_{+1}^{o,-}(\Lambda) - \hat{\mu}_{-1}^{o,+}(\Lambda), \quad \hat{\tau}^{o,+}(\Lambda) := \hat{\mu}_{+1}^{o,+}(\Lambda) - \hat{\mu}_{-1}^{o,-}(\Lambda).$$

5.2. A greedy algorithm

Although (9) is a linear program, its special structure admits a closed-form solution. The feasible set is a polytope defined by box constraints plus a single equality constraint (normalization). A standard result in linear programming implies that extreme points of this polytope have at most one coordinate strictly between its bounds—all other coordinates are either Λ^{-1} or Λ . Combined with the threshold structure from Section 4.2, this means the optimal solution assigns maximum weight Λ to the largest outcomes and minimum weight Λ^{-1} to the smallest, with at most one outcome receiving an intermediate weight to satisfy normalization.

This leads to a simple greedy algorithm. Sort the outcomes in treatment arm a in ascending order: $Y_{(1)}^r \leq Y_{(2)}^r \leq \dots \leq Y_{(n_a)}^r$, with corresponding baseline weights $p_{(1)}^{(a)}, \dots, p_{(n_a)}^{(a)}$. Initialize all reweighted probabilities at their lower bound: $q_{(j)}^{\text{low}} := p_{(j)}^{(a)} \Lambda^{-1}$. The total mass at the lower bound is Λ^{-1} , leaving a “budget” of $B := 1 - \Lambda^{-1}$ to distribute. Each outcome j can absorb additional mass up to its capacity $C_{(j)} := p_{(j)}^{(a)} (\Lambda - \Lambda^{-1})$.

To maximize the mean, allocate the budget starting from the largest outcome: fill $q_{(n_a)}$ to capacity, then $q_{(n_a-1)}$, and so on until the budget is exhausted. To minimize the mean, allocate starting from the smallest outcome. The following theorem confirms this procedure is optimal.

Algorithm 1: Outcome-shift sensitivity bounds

Input: Trial data $\{(X_i^r, A_i^r, Y_i^r)\}_{i=1}^{n^r}$, weights \hat{w}_i , $\Lambda \geq 1$
Output: Bounds $[\hat{\tau}^{o,-}, \hat{\tau}^{o,+}]$ on target ATE
for $a \in \{-1, +1\}$ **do**
 $\mathcal{I}_a \leftarrow \{i : A_i^r = a\}$, $n_a \leftarrow |\mathcal{I}_a|$;
 $p_i^{(a)} \leftarrow \hat{w}_i / \sum_{j \in \mathcal{I}_a} \hat{w}_j$ for $i \in \mathcal{I}_a$;
 Sort: $Y_{(1)}^r \leq \dots \leq Y_{(n_a)}^r$ with weights $p_{(j)}^{(a)}$;
 for $j = 1, \dots, n_a$ **do**
 $q_{(j)}^{\text{low}} \leftarrow p_{(j)}^{(a)} \Lambda^{-1}$, $C_{(j)} \leftarrow p_{(j)}^{(a)} (\Lambda - \Lambda^{-1})$;
 end
 $B \leftarrow 1 - \Lambda^{-1}$, $q^{\text{max}} \leftarrow q^{\text{low}}$;
 for $j = n_a$ **to** 1 **do**
 $\delta \leftarrow \min\{C_{(j)}, B\}$;
 $q_{(j)}^{\text{max}} += \delta$, $B -= \delta$;
 if $B = 0$ **then break**;
 end
 $\hat{\mu}_a^{o,+} \leftarrow \sum_{j=1}^{n_a} q_{(j)}^{\text{max}} Y_{(j)}^r$;
 $B \leftarrow 1 - \Lambda^{-1}$, $q^{\text{min}} \leftarrow q^{\text{low}}$;
 for $j = 1$ **to** n_a **do**
 $\delta \leftarrow \min\{C_{(j)}, B\}$;
 $q_{(j)}^{\text{min}} += \delta$, $B -= \delta$;
 if $B = 0$ **then break**;
 end
 $\hat{\mu}_a^{o,-} \leftarrow \sum_{j=1}^{n_a} q_{(j)}^{\text{min}} Y_{(j)}^r$;
end
return $\hat{\tau}^{o,-} = \hat{\mu}_{+1}^{o,-} - \hat{\mu}_{-1}^{o,+}$,
 $\hat{\tau}^{o,+} = \hat{\mu}_{+1}^{o,+} - \hat{\mu}_{-1}^{o,-}$

Theorem 5 (Greedy algorithm) Let $Y_{(1)}^r \leq \dots \leq Y_{(n_a)}^r$ be the sorted outcomes in arm a with baseline weights $p_{(j)}^{(a)}$. Define $q_{(j)}^{\text{low}} := p_{(j)}^{(a)} \Lambda^{-1}$, $C_{(j)} := p_{(j)}^{(a)} (\Lambda - \Lambda^{-1})$, and $B := 1 - \Lambda^{-1}$.

(Upper bound) Set $q_{(j)}^{\text{max}} := q_{(j)}^{\text{low}}$ for all j . For $j = n_a, n_a-1, \dots, 1$: set $\delta_{(j)} := \min\{C_{(j)}, B\}$, update $q_{(j)}^{\text{max}} \leftarrow q_{(j)}^{\text{max}} + \delta_{(j)}$ and $B \leftarrow B - \delta_{(j)}$; stop when $B = 0$. Then $\hat{\mu}_a^{o,+}(\Lambda) = \sum_{j=1}^{n_a} q_{(j)}^{\text{max}} Y_{(j)}^r$.

(Lower bound) Reset $B := 1 - \Lambda^{-1}$ and $q_{(j)}^{\text{min}} := q_{(j)}^{\text{low}}$. For $j = 1, 2, \dots, n_a$: set $\delta_{(j)} := \min\{C_{(j)}, B\}$, update $q_{(j)}^{\text{min}} \leftarrow q_{(j)}^{\text{min}} + \delta_{(j)}$ and $B \leftarrow B - \delta_{(j)}$; stop when $B = 0$. Then $\hat{\mu}_a^{o,-}(\Lambda) = \sum_{j=1}^{n_a} q_{(j)}^{\text{min}} Y_{(j)}^r$. The proof is presented in Appendix A.3.

The algorithm requires $O(n_a \log n_a)$ time for sorting plus $O(n_a)$ for the greedy allocation, giving overall complexity $O(n^r \log n^r)$. Algorithm 1 summarizes the complete procedure.

5.3. Consistency

The sample bounds are consistent for their population counterparts under standard regularity conditions.

Theorem 6 (Consistency) Suppose Assumption 1 holds, $|Y| \leq C$ almost surely, and the generalization weights satisfy $\hat{w}_i = w(X_i^r) + o_p(1)$ uniformly, where $w(x) = dP^o/dP^r(x)$ is bounded and strictly positive on the support of $P^{r,X}$. Then as $n^r, n^o \rightarrow \infty$, $\hat{\mu}_a^{o,\pm}(\Lambda) \xrightarrow{p} \mu_a^{o,\pm}(\Lambda)$, $\hat{\tau}^{o,\pm}(\Lambda) \xrightarrow{p} \tau^{o,\pm}(\Lambda)$, for each $a \in \{-1, +1\}$. The sample identified set $[\hat{\tau}^{o,-}(\Lambda), \hat{\tau}^{o,+}(\Lambda)]$ converges in Hausdorff distance to the population identified set $[\tau^{o,-}(\Lambda), \tau^{o,+}(\Lambda)]$. The proof is provided in Appendix A.4.

6. Experiments

We evaluate the proposed bounds via simulation, examining coverage, sharpness, and comparison to alternatives. We use four data-generating processes (DGPs) with unmeasured effect modification: DGP 1 (linear Gaussian), DGP 2 (nonlinear), DGP 3 (binary outcomes), and DGP 4 (heavy-tailed errors). Full DGP specifications, additional experiments, and extended results appear in Appendix B.

6.1. Sensitivity Envelopes

Figure 1 displays sensitivity envelopes—the sharp bounds as a function of Λ —for a single large dataset ($n^r = 2000, n^o = 5000$) from each DGP. As Λ increases from 1 (standard transportability), the identified set widens monotonically. The true target ATE falls within the bounds once Λ is sufficiently large. Binary outcomes (DGP 3) yield notably tighter intervals due to bounded support, while heavy-tailed errors (DGP 4) produce wider intervals for the same Λ .

6.2. Coverage and Sharpness

We assess repeated-sampling properties using DGP 1 with $(n^r, n^o) = (500, 1000)$ and $R = 1000$ replications. Figure 2 shows coverage and mean interval width as functions of Λ . At $\Lambda = 1$, coverage is near zero because transportability is violated. Coverage increases smoothly, reaching 0.98 at $\Lambda = 1.4$ and 1.00 by $\Lambda = 1.6$. The bounds are sharp: the sharpness ratio (finite-sample width divided by large- n oracle width) exceeds 0.98 across the Λ grid (Table 1).

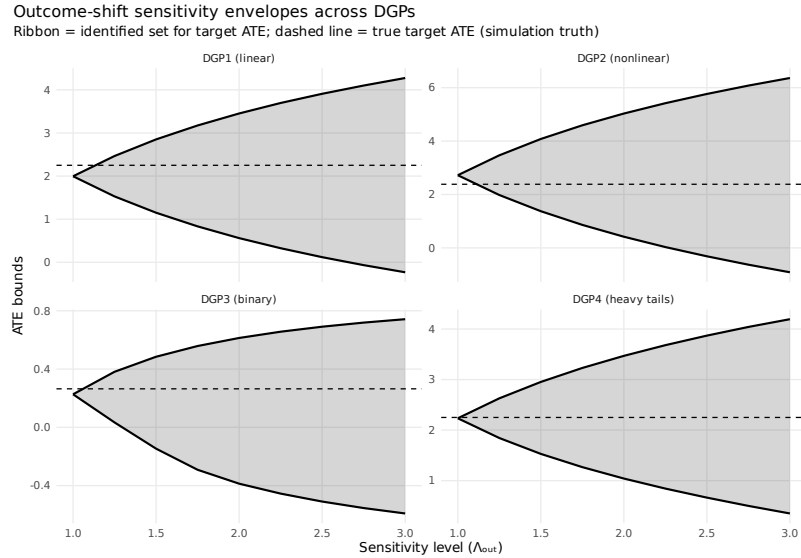


Figure 1: Sensitivity envelopes for DGPs 1–4. Each panel shows the sharp bound interval $[\hat{\tau}^{\sigma,-}(\Lambda), \hat{\tau}^{\sigma,+}(\Lambda)]$ as Λ varies, with the true target ATE marked. Binary outcomes (DGP 3) yield tighter bounds.

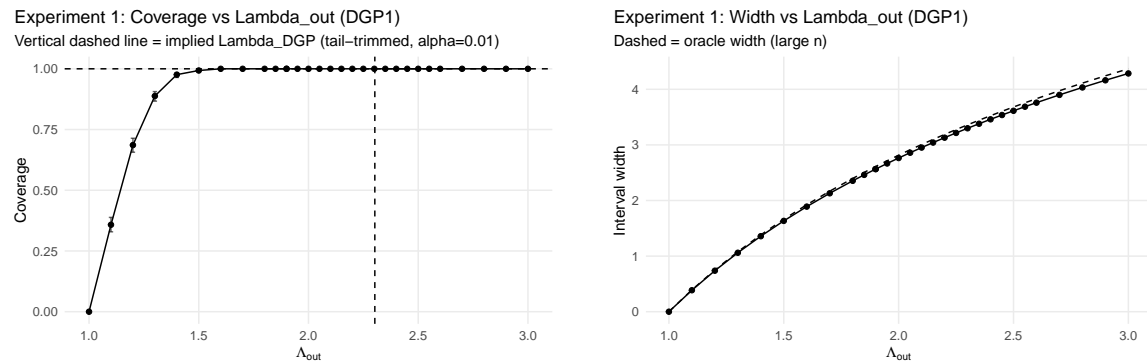


Figure 2: Coverage (left) and mean width (right) vs. Λ for DGP 1 ($R = 1000$). Coverage transitions from undercoverage at $\Lambda = 1$ to nominal levels by $\Lambda \approx 1.5$. Oracle width (dashed) confirms sharpness.

6.3. Comparison to Alternatives

We compare our sharp bounds to three alternatives: (i) the naive transported point estimate ($\Lambda = 1$), (ii) a nonparametric bootstrap CI for the transported estimator, and (iii) worst-case bounds assuming only bounded outcomes. Figure 3 presents results for DGP 1 at $\Lambda = 2.0$ with $R = 500$ replications. The naive point estimate achieves 0% coverage. The bootstrap CI achieves approximately 70% coverage with width 0.80, correctly quantifying sampling but not identification uncertainty. Our sharp bounds achieve 100% coverage with width 2.76. Worst-case bounds also achieve 100% coverage but with width 14.6—over five times wider—demonstrating the value of the structured sensitivity model.

Table 1: Selected operating points for DGP 1 ($R = 1000$). Sharpness ratio confirms finite-sample bounds approximate population bounds.

| Λ | Coverage | Mean width | Oracle width | Sharpness |
|-----------|----------|------------|--------------|-----------|
| 1.4 | 0.976 | 1.358 | 1.382 | 0.983 |
| 1.5 | 0.993 | 1.633 | 1.662 | 0.983 |
| 2.0 | 1.000 | 2.764 | 2.815 | 0.982 |

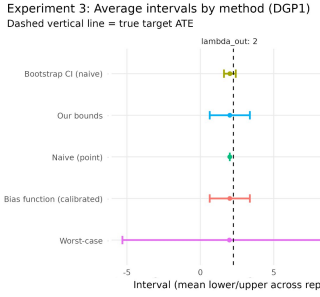


Figure 3: Comparison at $\Lambda = 2.0$ for DGP 1. Naive estimator and bootstrap CI fail to cover; worst-case bounds are uninformatively wide.

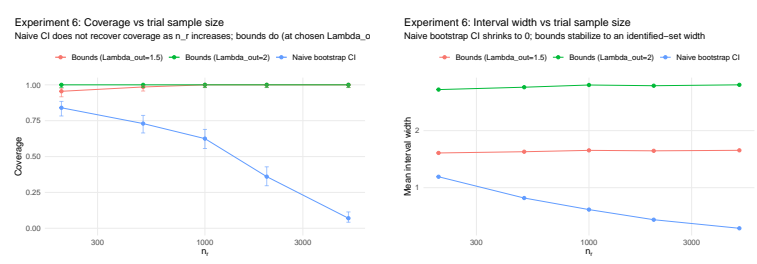


Figure 4: Identification vs. estimation (DGP 1). As n^r grows, naive bootstrap CI shrinks but coverage *worsens* (left). Sharp bounds maintain coverage with stable widths (right).

6.4. Identification vs. Estimation

A key conceptual point is that the limitation under violated transportability is *identification*, not estimation. We fix DGP 1 with $n^o = 5000$ and vary $n^r \in \{200, 500, 1000, 2000, 5000\}$ over $R = 200$ replications. Figure 4 shows a striking pattern: as n^r grows, the naive bootstrap CI shrinks but coverage *worsens*, dropping from approximately 50% at $n^r = 200$ to under 10% at $n^r = 5000$. The estimator becomes precisely wrong. Our sharp bounds (at $\Lambda = 2.0$) maintain near-perfect coverage with widths that stabilize rather than collapse—exactly the behavior expected under partial identification.

6.5. Robustness Across Outcome Types

Table 2 summarizes coverage and width across all four DGPs at $\Lambda = 2.0$. The method achieves near-nominal coverage in each case. Binary outcomes (DGP 3) yield the tightest intervals due to bounded support. Nonlinear effect modification (DGP 2) and heavy tails (DGP 4) require somewhat wider intervals, but coverage remains high, suggesting robustness to diverse outcome distributions.

Table 2: Coverage and width at $\Lambda = 2.0$ across DGPs ($R = 1000$). Complete results are provided in Appendix Table 7.

| DGP | Cov. | Width |
|------------------|-------|-------|
| 1 (Linear) | 1.000 | 2.769 |
| 2 (Nonlinear) | 1.000 | 4.260 |
| 3 (Binary) | 1.000 | 0.977 |
| 4 (Heavy-tailed) | 1.000 | 2.545 |

7. Conclusion

We developed a sensitivity analysis framework for generalizing treatment effects when transportability may fail due to unmeasured effect modifiers, bounding the likelihood ratio between target and

trial outcome densities by a parameter Λ to obtain sharp identified sets. The key insight is that extremal distributions have a threshold structure—optimal likelihood ratios take only boundary values Λ^{-1} and Λ —enabling a closed-form $O(n \log n)$ greedy algorithm. Simulations confirm nominal coverage when Λ encompasses the true shift, sharpness in finite samples, substantially tighter intervals than worst-case bounds, and correct diagnosis of violated transportability as an identification (not estimation) problem.

References

Elias Bareinboim and Judea Pearl. Causal inference and the data-fusion problem. *Proceedings of the National Academy of Sciences*, 113(27):7345–7352, 2016. doi: 10.1073/pnas.1510507113. URL <https://doi.org/10.1073/pnas.1510507113>.

Bénédicte Colnet, Imke Mayer, Guanhua Chen, Awa Dieng, Ruohong Li, Gaël Varoquaux, Jean-Philippe Vert, Julie Josse, and Shu Yang. Causal inference methods for combining randomized trials and observational studies: A review. *Statistical Science*, 39(1), 2024. doi: 10.1214/23-sts889. URL <https://doi.org/10.1214/23-sts889>.

Issa J. Dahabreh and Miguel A. Hernán. Extending inferences from a randomized trial to a target population. *European Journal of Epidemiology*, 34(8):719–722, 2019. doi: 10.1007/s10654-019-00533-2.

Issa J Dahabreh, Sébastien J-P A Haneuse, James M Robins, Sarah E Robertson, Ashley L Buchanan, Elizabeth A Stuart, and Miguel A Hernán. Study designs for extending causal inferences from a randomized trial to a target population. *American Journal of Epidemiology*, 190(8):1632–1642, 2020. doi: 10.1093/aje/kwaa270. URL <https://doi.org/10.1093/aje/kwaa270>.

Issa J. Dahabreh, James M. Robins, Sébastien J.-P. A. Haneuse, Iman Saeed, Sarah E. Robertson, Elizabeth A. Stuart, and Miguel A. Hernán. Sensitivity analysis using bias functions for studies extending inferences from a randomized trial to a target population. *Statistics in Medicine*, 42(13):2029–2043, 2023. doi: 10.1002/sim.9550. URL <https://doi.org/10.1002/sim.9550>.

Irina Degtyar and Sherri Rose. A review of generalizability and transportability. *Annual Review of Statistics and Its Application*, 10(1):501–524, 2023. doi: 10.1146/annurev-statistics-042522-103837. URL <https://doi.org/10.1146/annurev-statistics-042522-103837>.

Jacob Dorn and Kevin Guo. Sharp sensitivity analysis for inverse propensity weighting via quantile balancing. *Journal of the American Statistical Association*, 118(544):2645–2657, 2022. doi: 10.1080/01621459.2022.2069572. URL <https://doi.org/10.1080/01621459.2022.2069572>.

Alexander M. Franks, Alexander D’Amour, and Avi Feller. Flexible sensitivity analysis for observational studies without observable implications. *Journal of the American Statistical Association*, 115(532):1730–1746, 2020. doi: 10.1080/01621459.2019.1604369.

Dennis Frauen, Valentyn Melnychuk, and S. Feuerriegel. Sharp bounds for generalized causal sensitivity analysis, 2023. URL <https://www.semanticscholar.org/paper/72787ced723163d917f6fc2f84f8da6f8e461099>.

Melody Y Huang. Sensitivity analysis for the generalization of experimental results. *Journal of the Royal Statistical Society Series A: Statistics in Society*, 187(4):900–918, 2024. doi: 10.1093/jrsssa/qnae012. URL <https://doi.org/10.1093/jrsssa/qnae012>.

Albee Y. Ling, Maria E. Montez-Rath, Paulo Carita, Karen J. Chandross, Laurence Lucats, Zhaoling Meng, Bernard Sebastien, Kris Kapphahn, and Manisha Desai. An overview of current methods for real-world applications to generalize or transport clinical trial findings to target populations of interest. *Epidemiology*, 34(5):627–636, 2023. doi: 10.1097/ede.0000000000001633. URL <https://doi.org/10.1097/ede.0000000000001633>.

Trang Quynh Nguyen, Benjamin Ackerman, Ian Schmid, Stephen R. Cole, and Elizabeth A. Stuart. Sensitivity analyses for effect modifiers not observed in the target population when generalizing treatment effects from a randomized controlled trial: Assumptions, models, effect scales, data scenarios, and implementation details. *PLOS ONE*, 13(12):e0208795, 2018. doi: 10.1371/journal.pone.0208795. URL <https://doi.org/10.1371/journal.pone.0208795>.

Judea Pearl and Elias Bareinboim. Transportability of causal and statistical relations: A formal approach. In *Proceedings of the 25th AAAI Conference on Artificial Intelligence*, pages 247–254, 2011.

Paul R. Rosenbaum. *Observational Studies*. Springer-Verlag, New York, 2nd edition, 2002.

Elizabeth A. Stuart, Stephen R. Cole, Catherine P. Bradshaw, and Philip J. Leaf. The use of propensity scores to assess the generalizability of results from randomized trials. *Journal of the Royal Statistical Society: Series A (Statistics in Society)*, 174(2):369–386, 2011. doi: 10.1111/j.1467-985X.2010.00673.x.

Zhiqiang Tan. A distributional approach for causal inference using propensity scores. *Journal of the American Statistical Association*, 101(476):1619–1637, 2006. doi: 10.1198/016214506000000023. URL <https://doi.org/10.1198/016214506000000023>.

Qingyan Zhao, Dylan S. Small, and Bhaswar B. Bhattacharya. Sensitivity analysis for inverse probability weighting estimators via the percentile bootstrap. *Journal of the Royal Statistical Society Series B: Statistical Methodology*, 81(4):735–761, 2019. doi: 10.1111/rssb.12327. URL <https://doi.org/10.1111/rssb.12327>.

Appendix A. Proofs

A.1. Proof of Lemma 3

Write P for the conditional law of $Y \mid (A = a, X = x, S = r)$ on $[L, U]$, so $dP(y) = f^r(y \mid a, x) dy$. Consider the maximization problem; the minimization case is analogous with the ordering reversed.

Define the feasible set

$$\mathcal{C} := \left\{ r : [L, U] \rightarrow [\Lambda^{-1}, \Lambda] \mid \int r(y) dP(y) = 1 \right\}.$$

This set is convex and weak- \star compact in $L^\infty(P)$, and the objective $r \mapsto \int y r(y) dP(y)$ is linear and continuous, so a maximizer exists.

Step 1 (bang–bang/extreme-point structure). We claim that any extreme point of \mathcal{C} takes values in $\{\Lambda^{-1}, \Lambda\}$ P -a.s., possibly except on a P -null set. Indeed, if $r \in \mathcal{C}$ satisfies $\Lambda^{-1} < r(y) < \Lambda$ on a set E with $P(E) > 0$, we can choose measurable $E_1, E_2 \subseteq E$ with $P(E_1) = P(E_2) > 0$ and define for small $\epsilon > 0$,

$$r_\pm(y) := r(y) \pm \epsilon(\mathbf{1}_{E_1}(y) - \mathbf{1}_{E_2}(y)).$$

For ϵ small enough, $r_\pm \in \mathcal{C}$ and $r = (r_+ + r_-)/2$, so r is not extreme.

Step 2 (no inversions \Rightarrow threshold form). Let r be a maximizer that is an extreme point, hence $r(y) \in \{\Lambda^{-1}, \Lambda\}$ P -a.s. Define $H := \{y : r(y) = \Lambda\}$ and $Lw := \{y : r(y) = \Lambda^{-1}\}$. Suppose for contradiction that there exist $y_1 < y_2$ with $y_1 \in H$ and $y_2 \in Lw$, with both points belonging to sets of positive P -mass. Then there exist measurable sets $E_1 \subseteq H$ and $E_2 \subseteq Lw$ with $P(E_1) = P(E_2) > 0$ and such that $\sup E_1 < \inf E_2$ (take small neighborhoods and trim). Define \tilde{r} by swapping the values on E_1 and E_2 :

$$\tilde{r}(y) := \begin{cases} \Lambda^{-1}, & y \in E_1, \\ \Lambda, & y \in E_2, \\ r(y), & \text{otherwise.} \end{cases}$$

Then $\tilde{r} \in \mathcal{C}$ because $\int \tilde{r} dP = \int r dP$ (the swap changes the integral by $(\Lambda^{-1} - \Lambda)P(E_1) + (\Lambda - \Lambda^{-1})P(E_2) = 0$). Moreover, the objective strictly increases:

$$\int y \tilde{r}(y) dP(y) - \int y r(y) dP(y) = (\Lambda - \Lambda^{-1}) \left(\int_{E_2} y dP(y) - \int_{E_1} y dP(y) \right) > 0,$$

since all values in E_2 exceed all values in E_1 . This contradicts optimality.

Therefore, up to P -null sets, the set $H = \{r = \Lambda\}$ must be an upper tail: if $y \in H$ and $y' > y$, then $y' \in H$ P -a.s. Hence there exists a threshold $t \in [L, U]$ such that $r(y) = \Lambda$ for $y > t$ and $r(y) = \Lambda^{-1}$ for $y < t$, P -a.s.

Step 3 (atoms/ties at the threshold). If $P(\{t\}) = 0$, the normalization constraint determines t uniquely (up to null sets). If $P(\{t\}) > 0$, the normalization constraint may require assigning an intermediate value on the atom at t : set $r(t) = r_0 \in [\Lambda^{-1}, \Lambda]$ so that $\int r dP = 1$. This yields exactly the stated threshold form. \blacksquare

A.2. Proof of Theorem 4

Interval structure. Fix $a \in \{-1, +1\}$ and $x \in \mathcal{X}$. By Lemma 3, the conditional mean $\mu_a^o(x) = \int y r_a(x, y) f^r(y | a, x) dy$ is maximized and minimized over $\mathcal{R}_a(\Lambda)$ by threshold likelihood ratios, yielding the interval $[\mu_a^{o,-}(x; \Lambda), \mu_a^{o,+}(x; \Lambda)]$. Since the map $r_a \mapsto \mu_a^o(x)$ is linear and continuous, and the constraint set $\mathcal{R}_a(\Lambda)$ is convex and compact (in the weak- \star topology on L^∞), every value in this interval is attained by some admissible r_a .

For the marginal mean, we have

$$\mu_a^{o,+}(\Lambda) = \mathbb{E}^o[\mu_a^{o,+}(X; \Lambda)] = \int \mu_a^{o,+}(x; \Lambda) dP^{o,X}(x),$$

and similarly for $\mu_a^{o,-}(\Lambda)$. Since $|Y| \leq C$ almost surely, the conditional bounds satisfy $|\mu_a^{o,\pm}(x; \Lambda)| \leq C$ for all x , so the integrals are well-defined. The identified set for μ_a^o is thus $\mathcal{M}_a(\Lambda) = [\mu_a^{o,-}(\Lambda), \mu_a^{o,+}(\Lambda)]$.

For the target ATE, note that $\tau^o = \mu_{+1}^o - \mu_{-1}^o$ where μ_{+1}^o and μ_{-1}^o can be chosen independently (the likelihood ratios r_{+1} and r_{-1} are separate). Hence the identified set is

$$\mathcal{T}(\Lambda) = \{\mu_{+1}^o - \mu_{-1}^o : \mu_a^o \in \mathcal{M}_a(\Lambda), a \in \{-1, +1\}\} = [\mu_{+1}^{o,-} - \mu_{-1}^{o,+}, \mu_{+1}^{o,+} - \mu_{-1}^{o,-}].$$

Sharpness. Fix $a \in \{-1, +1\}$. Let r_a^+ and r_a^- be measurable maximizers/minimizers of the conditional problems (they exist by compactness/continuity as above), so that $\mathbb{E}^o[\mu_a^o(X; r_a^+)] = \mu_a^{o,+}(\Lambda)$ and $\mathbb{E}^o[\mu_a^o(X; r_a^-)] = \mu_a^{o,-}(\Lambda)$.

For any $\alpha \in [0, 1]$, define the convex combination

$$r_{a,\alpha}(x, y) := \alpha r_a^+(x, y) + (1 - \alpha) r_a^-(x, y).$$

Since the constraints defining $\mathcal{R}_a(\Lambda)$ are pointwise bounds and a linear normalization condition, $r_{a,\alpha} \in \mathcal{R}_a(\Lambda)$ for all $\alpha \in [0, 1]$. Moreover, the induced marginal mean is the corresponding convex combination:

$$\mathbb{E}^o[\mu_a^o(X; r_{a,\alpha})] = \alpha \mu_a^{o,+}(\Lambda) + (1 - \alpha) \mu_a^{o,-}(\Lambda).$$

Hence every μ_a^o in the interval $[\mu_a^{o,-}(\Lambda), \mu_a^{o,+}(\Lambda)]$ is attainable by choosing $\alpha = (\mu_a^o - \mu_a^{o,-})/(\mu_a^{o,+} - \mu_a^{o,-})$ (and any α if the endpoints coincide).

For the ATE, note r_{+1} and r_{-1} are chosen independently, so any pair (μ_{+1}^o, μ_{-1}^o) in the product of intervals is attainable, and therefore any difference $\tau = \mu_{+1}^o - \mu_{-1}^o$ in $[\tau^{o,-}(\Lambda), \tau^{o,+}(\Lambda)]$ is attainable. \blacksquare

A.3. Proof of Theorem 5

Work in q -variables: $q_{(j)} := p_{(j)}^{(a)} \lambda_{(j)}$. The constraints $\Lambda^{-1} \leq \lambda_{(j)} \leq \Lambda$ and $\sum_j p_{(j)}^{(a)} \lambda_{(j)} = 1$ are equivalent to

$$q_{(j)} \in [q_{(j)}^{\text{low}}, q_{(j)}^{\text{high}}], \quad \sum_{j=1}^{n_a} q_{(j)} = 1,$$

where $q_{(j)}^{\text{low}} := p_{(j)}^{(a)} \Lambda^{-1}$ and $q_{(j)}^{\text{high}} := p_{(j)}^{(a)} \Lambda$. The objective is $\sum_j q_{(j)} Y_{(j)}^r$.

Feasibility of the greedy construction. The algorithm starts at $q_{(j)}^{\text{low}}$ (which sums to Λ^{-1}) and distributes the remaining mass $\Delta_\Lambda = 1 - \Lambda^{-1}$ by adding at most $C_{(j)} = q_{(j)}^{\text{high}} - q_{(j)}^{\text{low}}$ to each coordinate, so the resulting q stays within the box constraints and sums to one.

Optimality (upper bound). Let q be any feasible point. Suppose there exist indices $i < j$ such that $Y_{(i)}^r < Y_{(j)}^r$, $q_{(i)} > q_{(i)}^{\text{low}}$, and $q_{(j)} < q_{(j)}^{\text{high}}$. Define

$$\varepsilon := \min\{q_{(i)} - q_{(i)}^{\text{low}}, q_{(j)}^{\text{high}} - q_{(j)}\} > 0,$$

and set $q'_{(i)} := q_{(i)} - \varepsilon$, $q'_{(j)} := q_{(j)} + \varepsilon$, leaving all other coordinates unchanged. Then q' remains feasible (sum preserved; still within bounds) and strictly improves the objective:

$$\sum_k q'_{(k)} Y_{(k)}^r - \sum_k q_{(k)} Y_{(k)}^r = \varepsilon (Y_{(j)}^r - Y_{(i)}^r) > 0.$$

Therefore, at any maximizer there cannot exist such a pair (i, j) : whenever a larger outcome j has not been filled to its upper bound, all smaller outcomes must sit at their lower bounds. This forces the “fill from the top” structure implemented by the greedy algorithm, with at most one partially filled coordinate (where the remaining mass runs out).

Optimality (lower bound). The minimization case is identical after reversing the ordering: if a smaller outcome has not been filled while a larger one has received extra mass above its lower bound, shifting mass downward decreases the objective. Hence the greedy “fill from the bottom” procedure is optimal. \blacksquare

A.4. Proof of Theorem 6

Fix $a \in \{-1, +1\}$ and $\Lambda \geq 1$. Let $\mathcal{I}_a = \{i : A_i^r = a\}$. Define the (arm-specific) weighted empirical measure of outcomes

$$\hat{P}_{n,a} := \sum_{i \in \mathcal{I}_a} p_i^{(a)} \delta_{Y_i^r}, \quad p_i^{(a)} := \frac{\hat{w}_i}{\sum_{j \in \mathcal{I}_a} \hat{w}_j}.$$

Let P_a^w denote the population analogue obtained by reweighting the trial arm- a distribution by the true density ratio $w(X) = dP^{o,X}/dP^{r,X}(X)$: for any Borel set $B \subseteq [-B, B]$,

$$P_a^w(B) := \frac{\mathbb{E}^r[w(X) \mathbf{1}\{A = a\} \mathbf{1}\{Y \in B\}]}{\mathbb{E}^r[w(X) \mathbf{1}\{A = a\}]}.$$

The denominator is strictly positive by positivity of $\mathbb{P}^r(A = a)$ and bounded, strictly positive w on the support of $P^{r,X}$.

Step 1: $\hat{P}_{n,a} \Rightarrow P_a^w$ (in a strong one-dimensional sense). Let $\tilde{p}_i^{(a)} := w(X_i^r)/\sum_{j \in \mathcal{I}_a} w(X_j^r)$ and $\tilde{P}_{n,a} := \sum_{i \in \mathcal{I}_a} \tilde{p}_i^{(a)} \delta_{Y_i^r}$. Uniform consistency $\sup_i |\hat{w}_i - w(X_i^r)| = o_p(1)$ and boundedness of w imply

$$\sum_{i \in \mathcal{I}_a} |p_i^{(a)} - \tilde{p}_i^{(a)}| = o_p(1), \quad \text{hence} \quad d_{\text{TV}}(\hat{P}_{n,a}, \tilde{P}_{n,a}) = o_p(1).$$

Moreover, since the weights $w(X)$ are bounded and the class $\{\mathbf{1}\{y \leq t\} : t \in \mathbb{R}\}$ is VC, a weighted Glivenko–Cantelli theorem yields

$$\sup_{t \in \mathbb{R}} \left| \tilde{P}_{n,a}((-\infty, t]) - P_a^w((-\infty, t]) \right| \xrightarrow{p} 0.$$

Because Y is supported on $[-B, B]$, uniform convergence of CDFs implies convergence in W_1 (Wasserstein-1) distance, and therefore $W_1(\hat{P}_{n,a}, P_a^w) \xrightarrow{p} 0$.

Step 2: continuity of the sharp-bound functionals. For any probability measure P supported on $[-B, B]$, define

$$\phi_{\Lambda}^+(P) := \sup_{\lambda: \Lambda^{-1} \leq \lambda \leq \Lambda, \int \lambda dP=1} \int y \lambda(y) dP(y), \quad \phi_{\Lambda}^-(P) := \inf_{\lambda: \Lambda^{-1} \leq \lambda \leq \Lambda, \int \lambda dP=1} \int y \lambda(y) dP(y).$$

The sample LP in (9) is exactly $\hat{\mu}_a^{o,\pm}(\Lambda) = \phi_{\Lambda}^{\pm}(\hat{P}_{n,a})$, and the population sharp bounds satisfy $\mu_a^{o,\pm}(\Lambda) = \phi_{\Lambda}^{\pm}(P_a^w)$.

Let $Q_P(u) := \inf\{y : P((-\infty, y]) \geq u\}$ be the generalized quantile function and set $\rho := 1/(\Lambda + 1)$. A standard rearrangement/knapsack argument (the continuous analogue of Theorem 5) gives the representation

$$\phi_{\Lambda}^+(P) = \Lambda^{-1} \int y dP(y) + (\Lambda - \Lambda^{-1}) \int_{1-\rho}^1 Q_P(u) du, \quad \phi_{\Lambda}^-(P) = \Lambda^{-1} \int y dP(y) + (\Lambda - \Lambda^{-1}) \int_0^{\rho} Q_P(u) du,$$

where the generalized quantile handles atoms and corresponds to allowing one partial weight at the threshold.

In one dimension, $W_1(P, Q) = \int_0^1 |Q_P(u) - Q_Q(u)| du$, and also $|\int y dP(y) - \int y dQ(y)| \leq W_1(P, Q)$ for measures on a bounded interval. Therefore,

$$|\phi_{\Lambda}^{\pm}(P) - \phi_{\Lambda}^{\pm}(Q)| \leq \Lambda W_1(P, Q),$$

so ϕ_{Λ}^{\pm} is continuous (indeed Lipschitz) in W_1 .

Combining with Step 1 yields $\hat{\mu}_a^{o,\pm}(\Lambda) = \phi_{\Lambda}^{\pm}(\hat{P}_{n,a}) \xrightarrow{p} \phi_{\Lambda}^{\pm}(P_a^w) = \mu_a^{o,\pm}(\Lambda)$.

Step 3: ATE bounds and Hausdorff convergence. By definition, $\hat{\tau}^{o,-}(\Lambda) = \hat{\mu}_{+1}^{o,-}(\Lambda) - \hat{\mu}_{-1}^{o,+}(\Lambda)$ and $\hat{\tau}^{o,+}(\Lambda) = \hat{\mu}_{+1}^{o,+}(\Lambda) - \hat{\mu}_{-1}^{o,-}(\Lambda)$, so convergence of the means implies $\hat{\tau}^{o,\pm}(\Lambda) \xrightarrow{p} \tau^{o,\pm}(\Lambda)$. Finally, for intervals on \mathbb{R} the Hausdorff distance equals the maximum endpoint error, hence

$$d_H([\hat{\tau}^{o,-}(\Lambda), \hat{\tau}^{o,+}(\Lambda)], [\tau^{o,-}(\Lambda), \tau^{o,+}(\Lambda)]) \xrightarrow{p} 0$$

■

Appendix B. Extended Simulation Study

This section empirically validates the outcome-shift sensitivity bounds, illustrates the coverage-informativeness tradeoff as the sensitivity parameter varies, and documents robustness to nonlinearity, discrete outcomes, heavy tails, and weight estimation.

B.1. Estimand, data structure, and sensitivity parameter

We consider a randomized trial conducted in a *trial population* (study indicator $S = r$) and a *target population* ($S = o$). In the trial we observe i.i.d. draws $\{(X_i, A_i, Y_i)\}_{i=1}^{n^r}$, where $A \in \{-1, +1\}$ is randomized with $\mathbb{P}(A = +1) = 1/2$, and in the target we observe baseline covariates $\{X_j\}_{j=1}^{n^o}$ (no outcomes).

The target estimand is the target average treatment effect (ATE)

$$\tau^o = \mathbb{E}[Y^o(+1) - Y^o(-1)],$$

where $Y^o(a)$ denotes the potential outcome under treatment level a in the target population.

Table 3: Simulation design summary (master table; can be trimmed).

| Exp. | Goal | DGP(s) | n^r | n^o | Reps | Key outputs |
|------|--|--------|-----------|-------|-----------|-----------------|
| Main | Envelopes vs. Λ_{out} | 1–4 | 2000 | 5000 | 1 dataset | Fig. 5 |
| 1 | Validation + sharpness | 1 | 500 | 1000 | 1000 | Fig. 6, Tab. 4 |
| 2 | Tradeoff vs. moderator shift | 1 | 500 | 1000 | 1000 | Fig. 7, Tab. 5 |
| 3 | Baseline comparison | 1 | 500 | 1000 | 50 | Fig. 8, Tab. 6 |
| 4 | Scaling in n^r (fixed Λ_{out}) | 1 | 100–5000 | 1000 | 300 | Fig. 9 |
| 5 | Robustness across outcome types | 1–4 | 500 | 1000 | 1000 | Fig. 10, Tab. 7 |
| 6 | Weight estimation sensitivity | 1 | 500 | 1000 | 150 | Fig. 11 |
| 6b | Identification vs estimation | 1 | 200–5000 | 5000 | 200 | Fig. 12 |
| 7 | Bounded-support DGP (LR holds literally) | 7 | 500 | 1000 | 200 | Fig. 13 |
| 8 | “Bang–bang” optimizer structure | 1 | 1 dataset | – | – | Fig. 14 |

Outcome-shift sensitivity model and Λ_{out} . The outcome-shift model in section 4 and theorem 2 constrains how much the *conditional outcome distribution* in the target can differ from the trial. In our simulation code and figures we denote the sensitivity parameter by $\Lambda_{\text{out}} \geq 1$ (this is the same Λ as in the main text, with an “out” subscript only to emphasize outcome shift). Concretely, for each treatment arm $a \in \{-1, +1\}$ and covariate profile x , we bound the conditional likelihood ratio by

$$\frac{1}{\Lambda_{\text{out}}} \leq \frac{f_{Y|A,X}^o(y \mid a, x)}{f_{Y|A,X}^r(y \mid a, x)} \leq \Lambda_{\text{out}} \quad \text{for all } y,$$

where $f_{Y|A,X}^s$ is the conditional outcome density/mass in population $s \in \{r, o\}$. When $\Lambda_{\text{out}} = 1$, this reduces to standard outcome transportability and the bounds collapse to the usual transported point estimate.

Generalization weights. To transport trial outcomes to the target covariate distribution we use inverse odds weights (see eq. (8)). In most experiments we use *oracle* weights $w(x) = f_X^o(x)/f_X^r(x)$ (available in simulation) to isolate outcome-shift effects from weight-estimation error. We separately study estimated weights in section B.9.

Metrics. Across Monte Carlo replications we report: (i) *coverage* of the true τ^o by the bound interval; (ii) *mean interval width*; (iii) a *sharpness ratio* defined as (sample mean width)/(oracle width), where “oracle width” is the width obtained by running the same procedure on an extremely large simulated trial to approximate the population sharp interval; and (iv) runtime where relevant. For coverage curves we include Wilson binomial intervals (where plotted; see tables for corresponding [lo, hi]).

B.2. Data-generating processes (DGPs 1–4)

All DGPs share a covariate shift between trial and target and an unmeasured moderator whose distribution differs across populations. Let $p = 5$ and write $X = (X_1, \dots, X_p)^\top$. We generate

$$X^r \sim \mathcal{N}(0_p, I_p), \quad X^o \sim \mathcal{N}(\mu_{\text{shift}} \cdot \mathbf{1}_p, I_p),$$

with $\mu_{\text{shift}} = 0.5$ in the main experiments. The unmeasured moderator satisfies

$$U^s \mid X \sim \mathcal{N}(\gamma_s X_1, 1), \quad s \in \{r, o\},$$

and we set $\gamma_r = 0$ and (unless otherwise stated) $\gamma_o = 0.5$, so that the target has a different distribution of the effect modifier even after conditioning on X .

DGP 1 (linear outcome with Gaussian moderator). Potential outcomes are

$$Y(a) = \beta_0 + \beta_x^\top X + a \cdot (\tau_0 + \beta_u U) + \varepsilon_a, \quad \varepsilon_a \sim \mathcal{N}(0, \sigma^2),$$

with $\beta_0 = 1$, $\beta_x = (0.3, 0.2, 0.1, 0.1, 0.1)^\top$, $\tau_0 = 1$, $\beta_u = 0.5$, and $\sigma = 1$. Because $A \in \{-1, +1\}$, the individual treatment effect is $Y(+1) - Y(-1) = 2(\tau_0 + \beta_u U)$, hence the target ATE has a closed form:

$$\tau^o = 2\tau_0 + 2\beta_u \mathbb{E}^o[U] = 2\tau_0 + 2\beta_u \gamma_o \mathbb{E}^o[X_1] = 2\tau_0 + 2\beta_u \gamma_o \mu_{\text{shift}} = 2 + \gamma_o \mu_{\text{shift}} = 2.25.$$

DGP 2 (nonlinear effect modification). Covariates and U are generated as in DGP 1, but the outcome model is nonlinear:

$$Y(a) = \beta_0 + \sin(\pi X_1/2) + X_2^2 + a \cdot \left(\tau_0 + \beta_u |U| \cdot \text{sign}(X_1) \right) + \varepsilon_a, \quad \varepsilon_a \sim \mathcal{N}(0, \sigma^2).$$

This preserves the same covariate shift and moderator shift but induces nonlinear treatment effect heterogeneity. The true τ^o is approximated via Monte Carlo with $n_{\text{truth}} = 10^6$ draws from the target joint distribution of (X, U) .

DGP 3 (binary outcomes). We generate binary outcomes via

$$Y(a) \sim \text{Bernoulli}(p_a(X, U)), \quad \text{logit}(p_a(X, U)) = \beta_0 + \beta_x^\top X + a \cdot (\tau_0 + \beta_u U),$$

with $\beta_0 = -0.5$, $\beta_x = (0.3, 0.2, 0.1, 0.1, 0.1)^\top$, $\tau_0 = 0.5$, and $\beta_u = 0.3$. The true τ^o is approximated via Monte Carlo with $n_{\text{truth}} = 10^6$ draws.

DGP 4 (heavy-tailed outcomes). This matches DGP 1 except the error is heavy-tailed:

$$Y(a) = \beta_0 + \beta_x^\top X + a \cdot (\tau_0 + \beta_u U) + \varepsilon_a, \quad \varepsilon_a \sim t_3 \text{ scaled to variance } \sigma^2,$$

so that rare large residuals occur. The closed-form τ^o remains the same as DGP 1.

B.3. Main envelope figure across DGPs

Before turning to repeated-sampling experiments, we plot a single-dataset “sensitivity envelope” for each DGP: the sharp lower and upper bounds as Λ_{out} varies, using a large trial ($n^r = 2000$) and target covariate sample ($n^o = 5000$). Figure 5 shows the expected monotone widening of the identified set as the analyst allows larger outcome shift. For bounded outcomes (DGP 3), widths are substantially smaller; for heavy tails (DGP 4), widths grow faster with Λ_{out} .

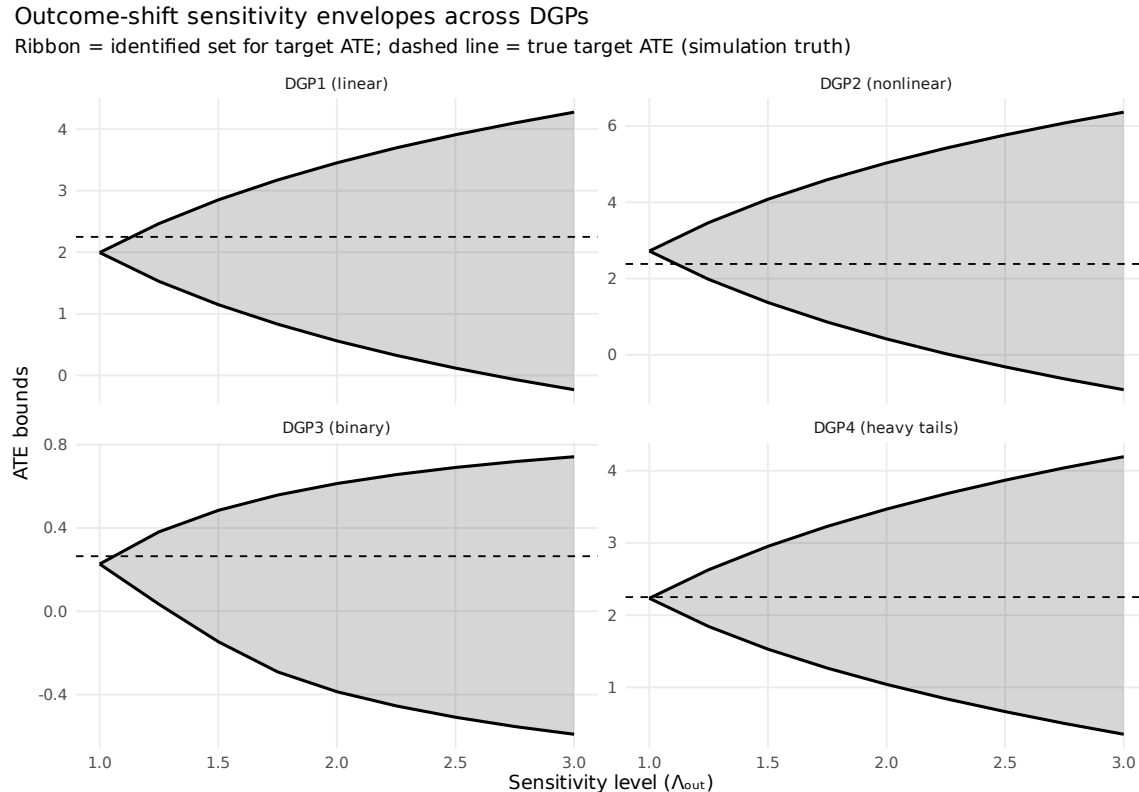


Figure 5: Sensitivity envelopes on a single large simulated dataset for DGPs 1–4. Each panel plots the sharp bound interval $[\hat{\tau}^-(\Lambda_{\text{out}}), \hat{\tau}^+(\Lambda_{\text{out}})]$ as a function of Λ_{out} , with the true target ATE indicated for reference. DGP 3 (binary outcomes) yields notably tighter envelopes due to bounded outcomes. [do we have sensitivity envelope term in the literature? highlighting null effect: zero line](#)

B.4. Experiment 1: validation and sharpness (DGP 1)

Design. We simulate DGP 1 with $(n^r, n^o) = (500, 1000)$ for $R = 1000$ replications. For each replication and each value on a grid $\Lambda_{\text{out}} \in [1, 3]$, we compute sharp bounds and record: coverage of $\tau^o = 2.25$, mean width, and a sharpness ratio relative to an ‘oracle width’ computed on an extremely large simulated dataset ($n^r = 100,000$) using the same procedure.

Because Gaussian likelihood ratios are technically unbounded, we also compute a *tail-trimmed* implied $\Lambda_{\text{DGP}}(\alpha)$ by restricting to central $(1 - \alpha)$ outcome mass (here $\alpha = 0.01$) and taking the smallest Λ that upper-bounds the conditional likelihood ratio on that truncated region. This provides a calibration reference (conservative for functionals like the ATE).

Results. Figure 6 shows a clean transition from severe undercoverage near $\Lambda_{\text{out}} = 1$ (transportability assumed) to near-nominal coverage once Λ_{out} is moderately above 1. Coverage is already ≈ 0.98 at $\Lambda_{\text{out}} = 1.4$ and ≈ 0.99 at $\Lambda_{\text{out}} = 1.5$, reaching 1.00 by $\Lambda_{\text{out}} = 1.6$. Importantly, widths closely track oracle widths: the sharpness ratio is about 0.98 across the grid (Tab. 4), indicating the finite-sample procedure is nearly as tight as the population sharp interval. The tipping point distribution in Figure 6 (rightmost panel) concentrates around $\Lambda_{\text{min}} \in [1.1, 1.3]$, the smallest sensitivity level needed for a given replicate to cover.

Table 4: Experiment 1 (DGP 1): selected operating points. Coverage is across $R = 1000$ replications; oracle widths use a large- n approximation.

| Λ_{out} | Coverage | Mean width | Oracle width | Sharpness ratio |
|------------------------|----------|------------|--------------|-----------------|
| 1.2 | 0.686 | 0.738 | 0.750 | 0.983 |
| 1.4 | 0.976 | 1.358 | 1.382 | 0.983 |
| 1.5 | 0.993 | 1.633 | 1.662 | 0.983 |
| 1.6 | 1.000 | 1.890 | 1.924 | 0.983 |
| 2.0 | 1.000 | 2.764 | 2.815 | 0.982 |
| 3.0 | 1.000 | 4.285 | 4.369 | 0.981 |

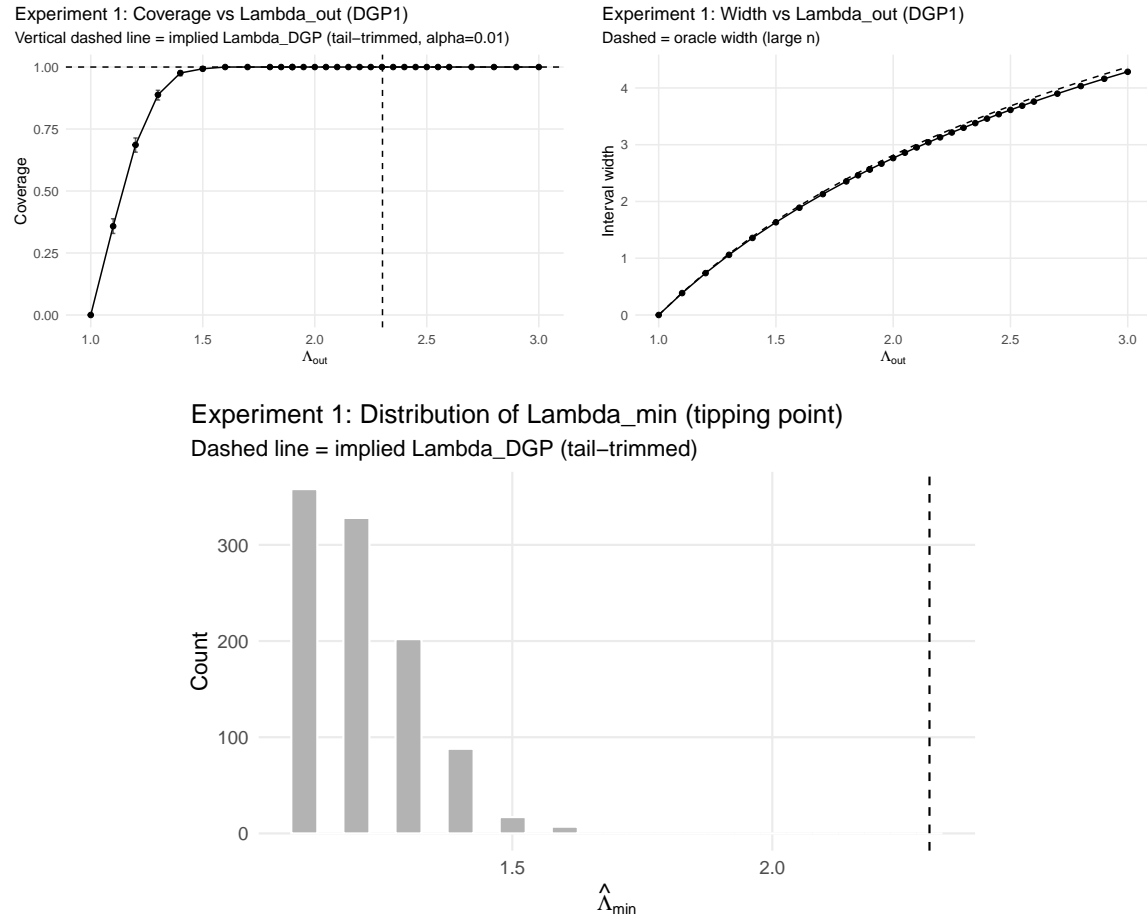


Figure 6: Experiment 1 (DGP 1): validation and sharpness. *Top-left*: coverage of the sharp interval for τ^o vs. Λ_{out} (with binomial uncertainty). *Top-right*: mean interval width vs. Λ_{out} , overlaid with an oracle large- n width. *Bottom*: distribution of $\hat{\Lambda}_{\text{min}}$, the smallest sensitivity level for which a replicate's interval covers τ^o .

B.5. Experiment 2: coverage–informativeness tradeoff vs. moderator shift (DGP 1)

Design. We vary the magnitude of population shift in the unmeasured moderator by setting $\gamma_o \in \{0.25, 0.5, 0.75, 1.0\}$ (with $\gamma_r = 0$), while keeping $(n^r, n^o) = (500, 1000)$ and $R = 1000$ replications.

Table 5: Experiment 2 (DGP 1): breakeven Λ_{out} (minimum achieving ≥ 0.95 coverage) as a function of moderator-shift strength γ_o . We also report the tail-trimmed $\Lambda_{\text{DGP}}(\alpha=0.01)$ computed from the conditional likelihood ratio, which is substantially more conservative for the ATE functional.

| γ_o | Breakeven Λ_{out} (95% cov.) | Tail-trimmed $\Lambda_{\text{DGP}}(0.01)$ |
|------------|---|---|
| 0.25 | 1.4 | 1.508 |
| 0.50 | 1.5 | 2.302 |
| 0.75 | 1.6 | 3.609 |
| 1.00 | 1.7 | 5.944 |

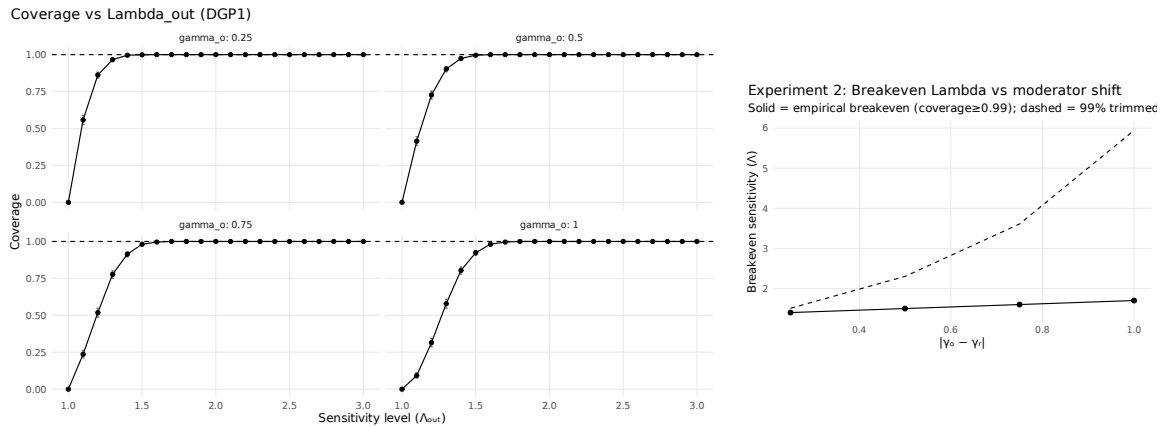


Figure 7: Experiment 2 (DGP 1): increasing moderator shift γ_o pushes the coverage-vs- Λ_{out} curve to the right. *Left:* coverage vs. Λ_{out} for $\gamma_o \in \{0.25, 0.5, 0.75, 1.0\}$. *Right:* breakeven Λ_{out} achieving 95% coverage.

tions. For each γ_o we sweep Λ_{out} and summarize the induced tradeoff between coverage and width. We also compute a *breakeven* sensitivity level, defined as the smallest Λ_{out} achieving at least 95% empirical coverage for that γ_o .

Results. As expected, increasing moderator shift makes transportability more fragile: the coverage curve shifts right, and the breakeven Λ_{out} rises nearly linearly with γ_o (Tab. 5, Figure 7). Concretely, the breakeven level increases from 1.4 at $\gamma_o = 0.25$ to 1.7 at $\gamma_o = 1.0$. This experiment provides an interpretable calibration: analysts can read off the sensitivity level needed to restore nominal coverage under a given degree of moderator shift.

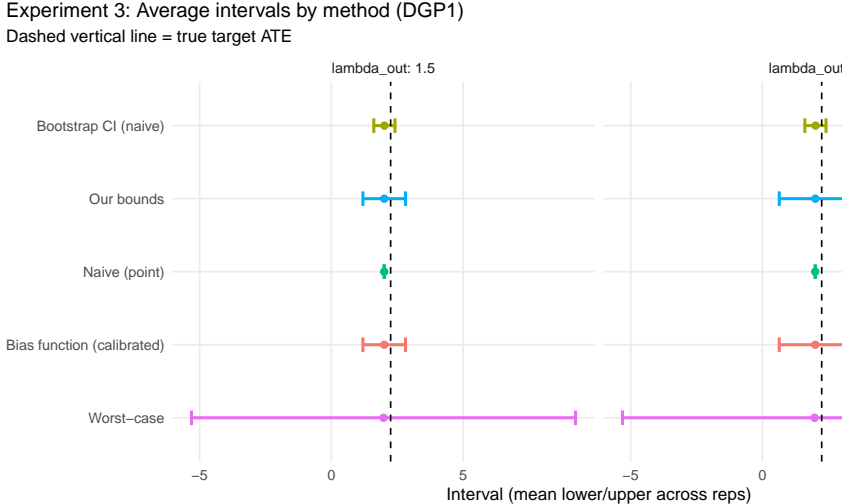
B.6. Experiment 3: comparison to baseline procedures (DGP 1)

Design. We compare our sharp bounds to common alternatives at two sensitivity levels $\Lambda_{\text{out}} \in \{1.5, 2.0\}$ on DGP 1 with $(n^r, n^o) = (500, 1000)$. The baselines are: (i) naive transported point estimate (assumes $\Lambda_{\text{out}} = 1$); (ii) naive nonparametric bootstrap CI for the transported estimator; (iii) a very conservative worst-case bound; and (iv) a calibrated bias-function baseline. (For computational convenience in this experiment, the run uses $R = 50$ replications; the gaps are large enough to be visually stable, and increasing R is straightforward.)

Results. The naive transported estimator (and its bootstrap CI) can be too optimistic: its intervals are narrow but under-cover, while worst-case bounds cover trivially but are far too wide. Our bounds

Table 6: Experiment 3 (DGP 1): baseline comparison at $\Lambda_{\text{out}} \in \{1.5, 2.0\}$. Coverage is across $R = 50$ replications.

| Method | Λ_{out} | Coverage | Mean width |
|--|------------------------|----------|------------|
| Naive (point, $\Lambda_{\text{out}}=1$) | 1.5 | 0.00 | 0.00 |
| Bootstrap CI (naive) | 1.5 | 0.70 | 0.804 |
| Our bounds | 1.5 | 0.98 | 1.616 |
| Worst-case | 1.5 | 1.00 | 14.576 |
| Naive (point, $\Lambda_{\text{out}}=1$) | 2.0 | 0.00 | 0.00 |
| Bootstrap CI (naive) | 2.0 | 0.70 | 0.804 |
| Our bounds | 2.0 | 1.00 | 2.734 |
| Worst-case | 2.0 | 1.00 | 14.576 |

Figure 8: Experiment 3 (DGP 1): forest plot comparing interval procedures at $\Lambda_{\text{out}} \in \{1.5, 2.0\}$. Our bounds remain informative while maintaining high coverage; worst-case bounds are orders of magnitude wider.

achieve near-nominal coverage with substantially smaller width than worst-case, and they coincide with the calibrated bias-function baseline here (Tab. 6).

B.7. Experiment 4: scaling with trial sample size (DGP 1)

Design. Fix $\Lambda_{\text{out}} = 2.0$ and ($n^o = 1000$), vary the trial size $n^r \in \{100, 200, 500, 1000, 2000, 5000\}$, and run $R = 300$ replications under DGP 1. We record coverage, mean width, sharpness ratio (relative to a large- n oracle width), and runtime.

Results. Figure 9 shows that width and sharpness stabilize quickly as n^r grows, while runtime remains negligible (milliseconds). Even at $n^r = 200$, coverage is already at 1.00 in this setting, and the sharpness ratio approaches 1 as finite-sample noise shrinks. This supports the practical usability of the greedy algorithm in algorithm 1.

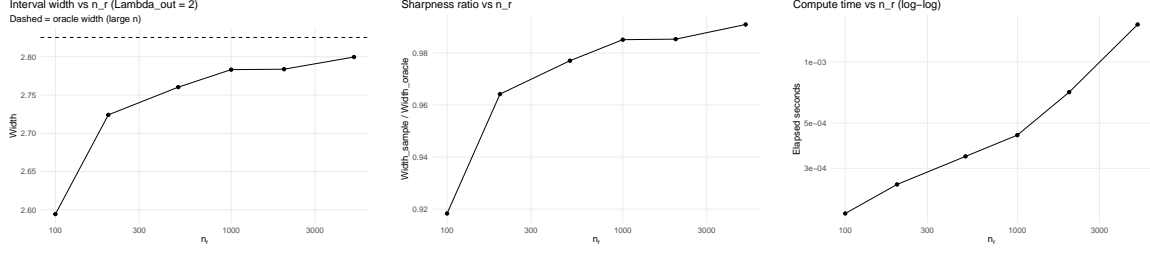


Figure 9: Experiment 4 (DGP 1): scaling with trial size n^r at fixed $\Lambda_{\text{out}} = 2$. *Left*: mean width vs. n^r . *Center*: sharpness ratio vs. n^r (approaches 1). *Right*: runtime vs. n^r (milliseconds).

Table 7: Experiment 5: coverage and width across DGPs.

| DGP | Λ_{out} | Coverage | Mean width |
|--------------------|------------------------|----------|------------|
| DGP1 (linear) | 1.5 | 0.991 | 1.635 |
| DGP1 (linear) | 2.0 | 1.000 | 2.769 |
| DGP1 (linear) | 3.0 | 1.000 | 4.296 |
| DGP2 (nonlinear) | 1.5 | 0.995 | 2.498 |
| DGP2 (nonlinear) | 2.0 | 1.000 | 4.260 |
| DGP2 (nonlinear) | 3.0 | 1.000 | 6.717 |
| DGP3 (binary) | 1.5 | 0.999 | 0.609 |
| DGP3 (binary) | 2.0 | 1.000 | 0.977 |
| DGP3 (binary) | 3.0 | 1.000 | 1.332 |
| DGP4 (heavy tails) | 1.5 | 0.989 | 1.497 |
| DGP4 (heavy tails) | 2.0 | 1.000 | 2.545 |
| DGP4 (heavy tails) | 3.0 | 1.000 | 3.991 |

B.8. Experiment 5: robustness across outcome types (DGPs 1–4)

Design. We run the same Monte Carlo experiment across DGPs 1–4 with $(n^r, n^o) = (500, 1000)$, $R = 1000$ replications, and $\Lambda_{\text{out}} \in \{1.5, 2.0, 3.0\}$.

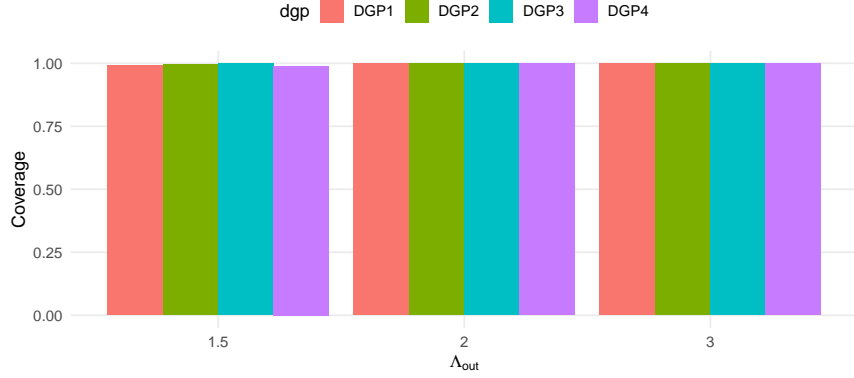
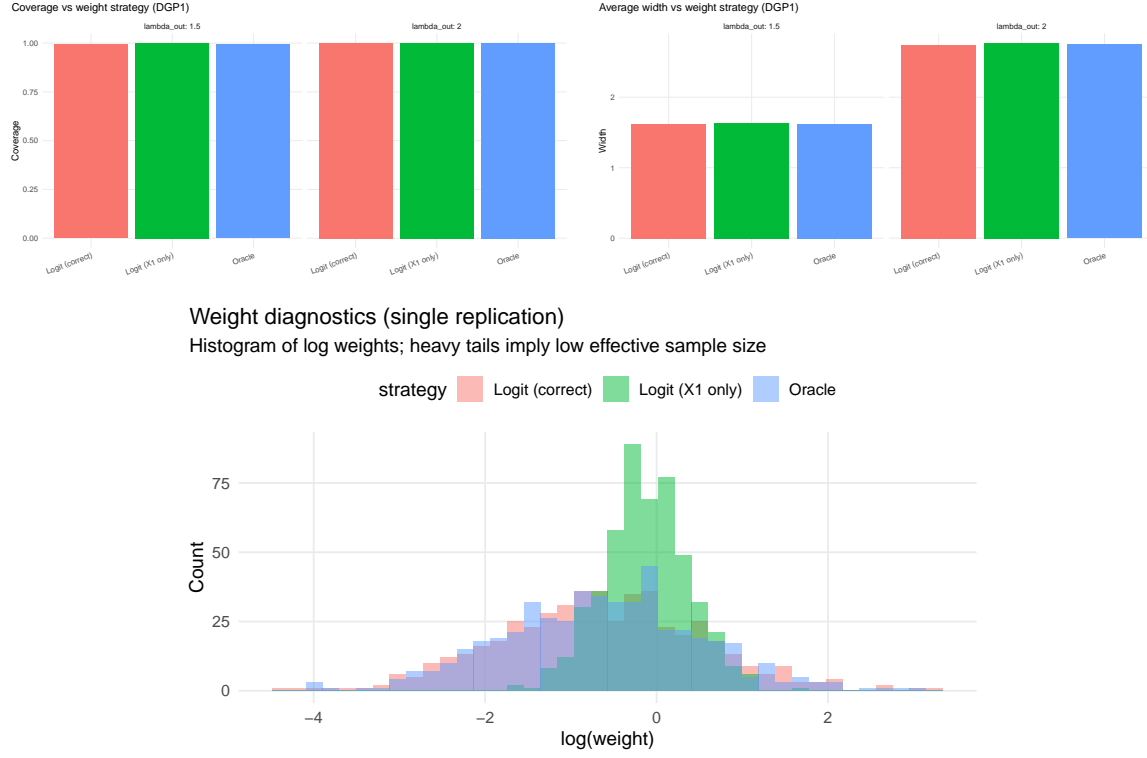
Results. Figure 10 and Tab. 7 show that the bounds maintain high coverage across nonlinear, binary, and heavy-tailed settings. Binary outcomes (DGP 3) yield the tightest intervals, while nonlinear and heavy-tailed outcomes require wider intervals for the same Λ_{out} , as expected.

B.9. Experiment 6: sensitivity to weight estimation (DGP 1)

Design. We compare three weighting strategies in DGP 1 with $(n^r, n^o) = (500, 1000)$ and $R = 150$ replications: (i) oracle weights using the known Gaussian density ratio; (ii) estimated logistic membership weights using the correct covariates; and (iii) a misspecified logistic membership model using only X_1 . We report coverage and width at $\Lambda_{\text{out}} \in \{1.5, 2.0\}$ and visualize the induced weight distributions.

Results. Figure 11 shows that (in this moderate covariate-shift setting) bounds are stable across weighting strategies: estimated weights closely match oracle performance, and even mild misspec-

Experiment 5: Coverage across DGPs

Figure 10: Experiment 5: robustness across DGPs 1–4. Coverage at $\Lambda_{\text{out}} = 1.5$ is already near nominal in all cases and reaches 1.00 by $\Lambda_{\text{out}} = 2.0$ by all DGPs.Figure 11: Experiment 6 (DGP 1): sensitivity to weight estimation. *Top-left*: coverage by weighting strategy. *Top-right*: width by weighting strategy. *Bottom*: weight distribution diagnostic (log-scale), illustrating tail behavior across strategies.

ification does not drastically change width or coverage at these Λ_{out} values. The weight histogram highlights how misspecification changes tail behavior (maximum weight and effective sample size), which is useful for diagnostics in applications.

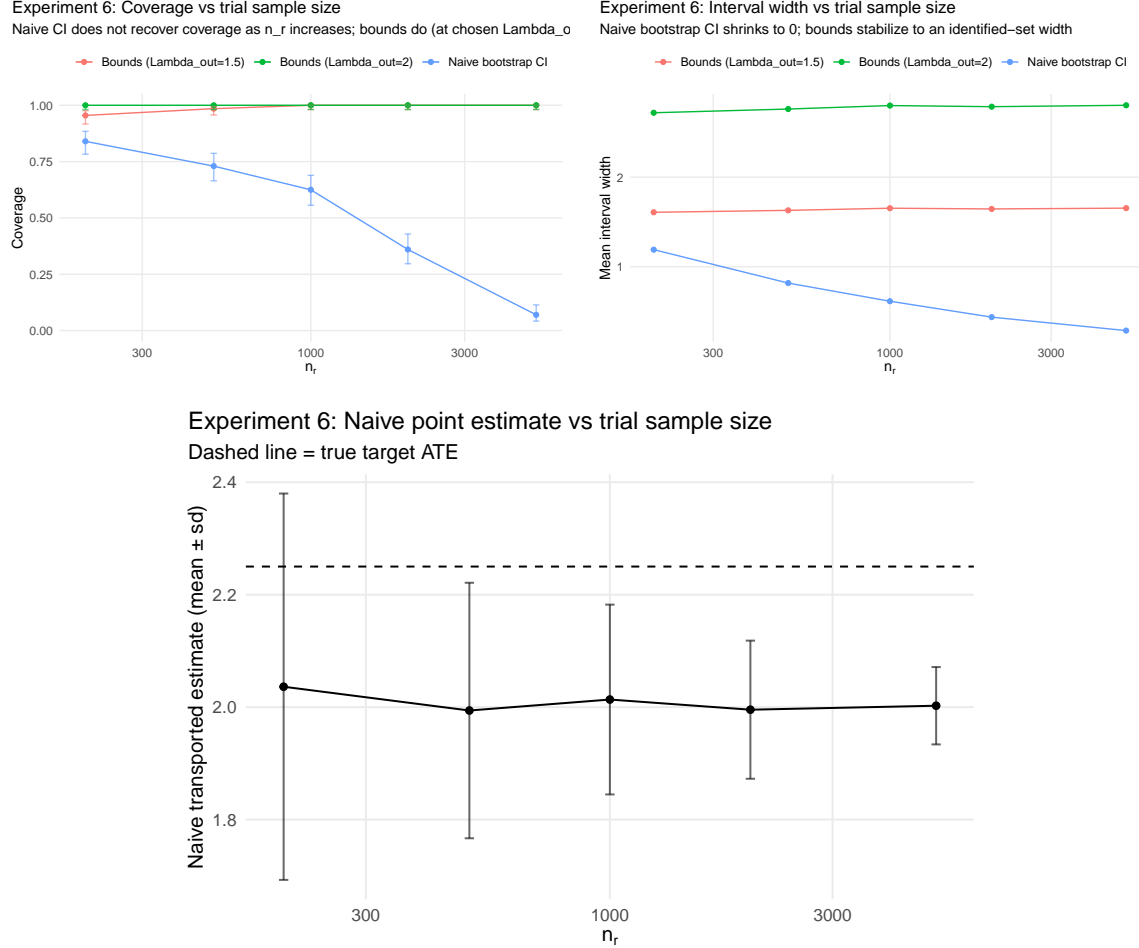


Figure 12: Experiment 6b (DGP 1): identification vs. estimation. As n^r grows, the naive bootstrap CI becomes narrower yet less valid, while sharp bounds retain coverage and stabilize in width. The bottom panel (optional) illustrates convergence of the naive point estimate away from the true τ^o .

B.10. Experiment 6b: identification vs. estimation scaling (DGP 1)

Design. This experiment isolates an important failure mode of naive inference: even with very large n^r , the transported point estimator can be *precisely wrong* when outcome transportability fails. We simulate DGP 1 with a large target covariate sample $n^o = 5000$, vary trial size $n^r \in \{200, 500, 1000, 2000, 5000\}$, and run $R = 200$ replications per n^r . We compare: (i) the naive transported point estimate (equivalently $\Lambda_{out} = 1$), (ii) a naive nonparametric bootstrap CI for the transported estimator (200 bootstrap resamples), and (iii) our sharp bounds at $\Lambda_{out} \in \{1.5, 2.0\}$.

Results. Figure 12 shows a stark pattern: as n^r increases, the naive bootstrap CI shrinks rapidly but coverage *worsens* (e.g., dropping to ≈ 0.07 by $n^r = 5000$), demonstrating that the dominant limitation is *identification*, not sample size. In contrast, the sharp bounds maintain near-nominal coverage with widths that do not collapse to zero (as expected under partial identification).

B.11. Experiment 7: bounded-support DGP where the LR model holds literally

A common technical concern is that for Gaussian outcomes the pointwise likelihood ratio can be unbounded. To demonstrate that our method behaves as intended when the model holds literally, we construct a bounded-support DGP (DGP 7) with truncated covariates and truncated outcomes so that the conditional likelihood ratio is finite.

DGP 7 definition (bounded). We draw covariates from truncated normals:

$$X^r \sim \text{TruncNormal}(0, I_p; [-B, B]^p), \quad X^o \sim \text{TruncNormal}(\delta \mathbf{1}_p, I_p; [-B, B]^p),$$

with $B = 3$ and $\delta = 0.5$. The moderator is generated as before with $\gamma_r = 0$ and $\gamma_o = 0.2$: $U^s \mid X \sim \mathcal{N}(\gamma_s X_1, 1)$. Outcomes follow a truncated normal:

$$Y(a) \sim \text{TruncNormal}\left(\beta_0 + \beta_x^\top X + a(\tau_0 + \beta_u U), \sigma^2; [y_L, y_U]\right),$$

with $\beta_0 = 1$, $\beta_x = (0.5, 0.3, 0.2, 0.1, 0.1)^\top$, $\tau_0 = 1$, $\beta_u = 0.25$, $\sigma = 1$, and $[y_L, y_U] = [-3, 3]$. For this DGP we also compute a literal global Λ_{DGP} by maximizing the conditional likelihood ratio over (a, x, y) on the bounded support (reported in the corresponding table file).

Design and results. We run an Exp-1-style sweep with $(n^r, n^o) = (500, 1000)$ and $R = 200$ replications over a grid of Λ_{out} . Figure 13 shows the same qualitative pattern as in DGP 1, but here the LR-bounded model is well-defined without trimming: coverage increases monotonically with Λ_{out} , and widths grow smoothly. The tipping points concentrate near $\Lambda_{\min} \approx 1.1$ in this particular setting.

B.12. Experiment 8: “bang–bang” tilting visualization

Finally, we visualize the structure predicted by theorem 3: the extremal solutions that attain the sharp upper/lower bounds correspond to multipliers that largely saturate at the LR constraints, producing a near-threshold (“bang–bang”) pattern when ordered by outcome (or the relevant sufficient statistic).

B.13. Summary discussion (what the simulations show)

Across DGPs and experimental designs, the simulations support four main conclusions. First, the proposed procedure achieves empirical coverage once Λ_{out} is large enough to plausibly contain the true outcome shift, and it transitions smoothly from the transported point estimate at $\Lambda_{\text{out}} = 1$ to wider partial-identification intervals as Λ_{out} increases (Exp. 1, Fig. 6). Second, the intervals are *sharp* in the sense that their widths closely match large- n oracle widths, implying little avoidable conservatism in finite samples (Exp. 1, Tab. 4). Third, the method exposes an explicit coverage–informativeness tradeoff and yields interpretable “breakeven” sensitivity levels under varying degrees of moderator shift (Exp. 2, Tab. 5). Fourth, the identification aspect is central: naive transported estimators can become arbitrarily precise yet invalid as n^r grows, whereas sharp bounds maintain coverage and do not collapse (Exp. 6b, Fig. 12). Robustness experiments (Exp. 5) and diagnostics around weight estimation (Exp. 6) further support practical applicability, while Exp. 7 and Exp. 8 address common technical and interpretability questions about LR-bounded models and the structure of the optimizing tilts.

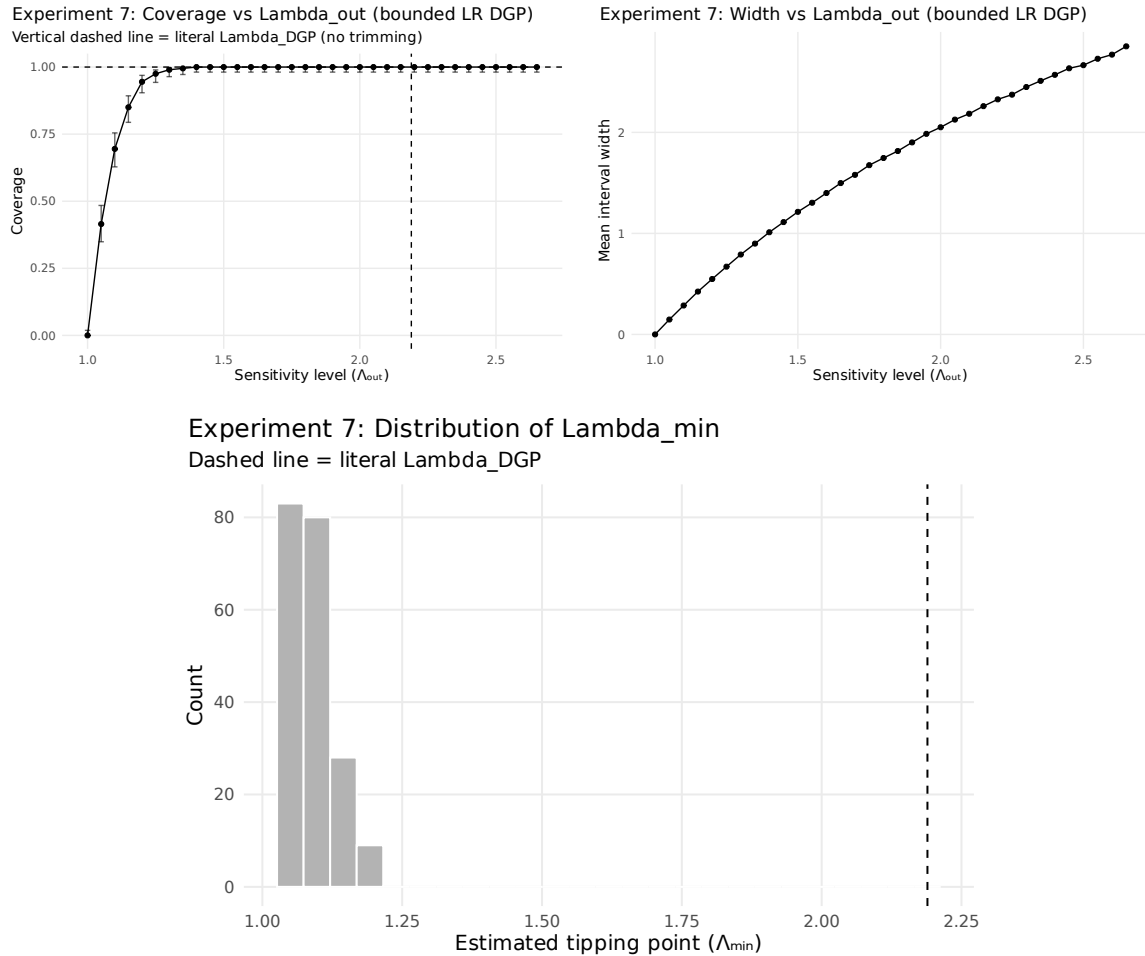


Figure 13: Experiment 7 (bounded-support DGP): when outcomes and covariates have bounded support, the pointwise LR model holds literally. Coverage increases with Λ_{out} and the tipping-point distribution is concentrated.

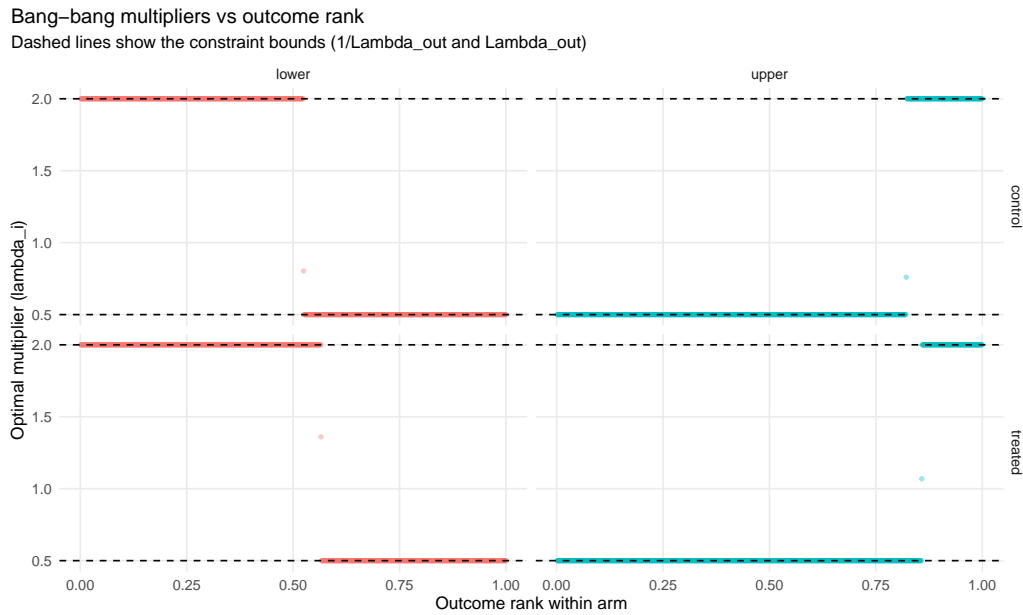


Figure 14: Experiment 8: “bang–bang” structure of the bound-attaining tilts. The estimated multipliers (density ratio adjustments) concentrate near the constraint values and switch sharply around a threshold, consistent with theorem 3.

